Neuroscience Applied

GPR101 loss promotes insulin resistance and diet-induced obesity risk

--Manuscript Draft--

Manuscript Number:	
Full Title:	GPR101 loss promotes insulin resistance and diet-induced obesity risk
Article Type:	Full Length Article
Keywords:	GPR101; Diet-induced obesity; insulin resistance; hypothalamus; inflammation
Corresponding Author:	Sabine M. Hölter, Ph.D. Helmholtz Center Munich German Research Center for Environmental Health GERMANY
Corresponding Author Secondary Information:	
Corresponding Author's Institution:	Helmholtz Center Munich German Research Center for Environmental Health
Corresponding Author's Secondary Institution:	
First Author:	Lillian Garrett, PhD
First Author Secondary Information:	
Order of Authors:	Lillian Garrett, PhD
	Martin Irmler
	Angela Baljuls
	Birgit Rathkolb
	Nathalia Dragano
	Raffaele Gerlini
	Adrián Sanz-Moreno
	Antonio Aguilar-Pimentel
	Lore Becker
	Markus Kraiger
	Rosa Reithmeir
	Johannes Beckers
	Julia Calzada-Wack
	Wolfgang Wurst
	Helmut Fuchs
	Valerie Gailus-Durner
	Tina Zimmermann
	Sabine M. Hölter
	Martin Hrabě de Angelis
Order of Authors Secondary Information:	
Abstract:	G-protein-coupled receptors (GPCRs) represent targets for improved low-side-effect therapies to tackle the evolving Western obesity epidemic. The orphan (o) GPCR GPR101 emerged as an attractive candidate in this regard. Expressed on cells in brain areas regulating energy homeostasis, including the hunger-suppressing proopiomelanocortin (POMC) + neurons, it is minimally expressed outside the brain. To understand the function of this receptor in vivo, we herein generated and

	comprehensively characterized a Gpr101 knockout mouse line, either under standard feeding conditions or with chronic high-fat diet (HFD) access (16 weeks). GPR101 loss accelerated the risk for diet-induced obesity (DIO), hyperinsulinemia and disrupted glucose homeostasis. Hypothalamic transcriptomic analysis revealed also decreased Pomc activation with HFD suggesting impaired hunger suppression. Moreover, on a standard diet, there was a molecular signature of downregulated tristetraprolin (TTP) pathway gene activation suggesting impaired inflammation resolution and one of aberrant microglial phagocytosis and lipid metabolism on HFD. Morphometry revealed altered hypothalamic arcuate nucleus microglial morphology consistent with the transcriptomic profile. We discuss how the GPR101 specialized pro-resolving mediator (SPM) receptor capacity likely underlies the aberrant microglial function and contributes to DIO risk. Thus, this evidence shows that GPR101 is a potential therapeutic target for DIO through, among other factors, effects on hypothalamic inflammation resolution.
Suggested Reviewers:	Ingo Bechmann Professor, Leipzig University ingo.bechmann@medizin.uni-leipzig.de Professor Bechmann is a microglia expert and so would be able to best judge the scientific credibility of our findings
	Yann Herault Professor, Institut of Genetics and Molecular and Cellular Biology yann.herault@igbmc.fr Professor Herault is an expert in genetic mouse models and neuropsychiatric disease modelling
	John Cryan Professor, University College Cork j.cryan@ucc.ie Professor Cryan is an expert in mouse models of brain control of feeding and metabolism and is therefore in a position to critically review the manuscript
	Carsten Wotjak Boehringer Ingelheim GmbH wotjak@psych.mpg.de
Opposed Reviewers:	
Additional Information:	
Question	**Response**

HELMHOLTZ MUNICH

Helmholtz Zentrum München Deutsches Forschungszentrum für
Gesundheit und Umwelt (GmbH), Postfach 11 29, 85758 Neuherberg

Prof. Andreas Meyer-Lindenberg, MD
Editor-in-chief Neuroscience Applied
Central Institute of Mental Health,
Mannheim, Germany

PD Dr. Sabine M. Hölter
Team Leader

+49 89 3187 3674
hoelter@helmholtz-munich.de

Manuscript submission

19. Dezember 2022

Dear Prof. Meyer-Lindenberg,

We are delighted to submit our manuscript entitled “GPR101 loss promotes insulin resistance and diet-induced obesity risk” for consideration as a research article in Neuroscience Applied. We believe that our manuscript will be of interest to your readers as we take a neuroscience-based approach to understanding diet-induced obesity (DIO) and, in so doing, highlight the therapeutic potential of the orphan G-protein coupled receptor GPR101.

In tackling the Western obesity epidemic, there is a need for novel and more efficacious therapies with minimal side effects. GPR101, predominantly expressed in the hypothalamus, alters appetite and energy expenditure through an unknown mechanism and thus has potential in this regard. Recent evidence also implicates this receptor in inflammation resolution through its pro-resolving mediator capacity. We showed here, for the first time, that loss of Gpr101 in mice augmented DIO and insulin resistance risk on high-fat diet (HFD). Furthermore, we established that there is a molecular signature of immune and microglial activation under standard conditions and microglial morphology indicative of blunted microglial phagocytosis with HFD. Combined, this work illustrates the potential of GPR101 as a novel target for DIO treatment through, among other factors, hypothalamic immune responsivity and resolution.

I would like to submit this article as the first contribution to the Special Section topic “Addressing pitfalls in translation” you invited me to put together as ECNP Preclinical Data Forum Network Chair. You can find a short introductory editorial to this topic on the second page of this letter.

Thank you for receiving the manuscript, it describes original work, is not under consideration for publication elsewhere and all authors approved the manuscript and declare no conflict of interest. I hope you will find it of interest, we appreciate your time and look forward to your response.

All the RNA-seq data generated for this study can be accessed here:
https://www.ncbi.nlm.nih.gov/geo/query/acc.cgi?acc=GSE220533 using the token mbsdmkuczbelpux.

With best wishes,

HELMHOLTZ MUNICH

ATTACHMENT: Introductory editorial to Special Section topic

Addressing pitfalls in translation

Translational failures in neuropsychiatry have been widely discussed for quite some time, prompting the development of several suggestions for solutions. Prominent solution suggestions include enhancement of preclinical study design and data quality, pre-registration of preclinical studies, and improved back-translation of clinical diagnoses for preclinical usage based on the RDoC framework.

This Special Section attempts to highlight less well-known solution suggestions that have been developed by PREMOS (Predictive Model Systems), a cluster supported by the European Brain Research Area (EBRA): European brain research: Addressing translational gaps (openaccessgovernment.org). They focus more on the facilitation of mechanistic insights and a better understanding of disease etiologies by broadening our perspective in disease-related investigations in animal models. For example, sex is still not systematically considered as a biological variable in basic neuroscience and preclinical studies, with potentially detrimental consequences for the translational success of the insights gained. Likewise, most studies are very focused instead of a broader consideration of multiple body systems that might be clinically relevant in the context of disease comorbidities. Similarly, including environmental factors like diets or genetic factors could enhance our mechanistic understanding as well as target identification.
The different contributions to this Special Section give individual examples for the inclusion of potential translationally relevant aspects that have largely been ignored in study designs in the past.

Declaration of interests

☐The authors declare that they have no known competing financial interests or personal relationships that could have appeared to influence the work reported in this paper.

☒The authors declare the following financial interests/personal relationships which may be considered as potential competing interests:

Martin Hrabe de Angelis reports was provided by German Federal Ministry of Education and Research (Infrafrontier grant 01KX1012).

GPR101 loss promotes insulin resistance and diet-induced obesity risk

Lillian Garrett[1,2], Martin Irmler[1], Angela Baljuls[10], Birgit Rathkolb[1,7,8], Nathalia Dragano[1], Raffaele Gerlini[1,7], Adrián Sanz-Moreno[1], Antonio Aguilar-Pimentel[1], Lore Becker[1], Markus Kraiger[1], Rosa Reithmeir[2,9], Johannes Beckers[1,6,7], Julia Calzada-Wack[1], Wolfgang Wurst[2,3,4,5], Helmut Fuchs[1], Valerie Gailus-Durner[1], Tina Zimmermann[10#], Sabine M. Hölter[1,2,9,#,*], Martin Hrabě de Angelis[1,6,7,#,*]

[1]Institute of Experimental Genetics and German Mouse Clinic, Helmholtz Zentrum München, German Research Center for Environmental Health, Neuherberg, Germany

[2]Institute of Developmental Genetics, Helmholtz Zentrum München, German Research Center for Environmental Health, Neuherberg, Germany

[3]Chair of Developmental Genetics, TUM School of Life Sciences, Technische Universität München, Freising-Weihenstephan, Germany

[4]Deutsches Institut für Neurodegenerative Erkrankungen (DZNE) Site Munich, Feodor-Lynen-Str. 17, 81377 Munich, Germany

[5]Munich Cluster for Systems Neurology (SyNergy), Adolf-Butenandt-Institut, Ludwig-Maximilians-Universität München, Feodor-Lynen-Str. 17, 81377 Munich, Germany

[6]Chair of Experimental Genetics, TUM School of Life Sciences, Technische Universität München, Alte Akademie 8, 85354 Freising, Germany

[7]German Center for Diabetes Research (DZD), Ingolstädter Landstr. 1, 85764 Neuherberg, Germany

[8]Institute of Molecular Animal Breeding and Biotechnology, Gene Center, Ludwig-Maximilians University Munich, Munich, Germany

[9]Technische Universität München, Freising-Weihenstephan, Germany

[10]Boehringer Ingelheim Pharma GmbH & Co. KG, Birkendorfer Straße 65, 88397 Biberach an der Riss, Germany

[#]These authors contributed equally

*Correspondence to:
Dr. Sabine M. Hölter
Institute of Developmental Genetics
Helmholtz Center Munich
Ingolstädter Landstr. 1
D-85764 Neuherberg, Germany
E-Mail: hoelter@helmholtz-muenchen.de

Prof. Martin Hrabě de Angelis
Institute of Experimental Genetics
Helmholtz Center Munich,
Ingolstädter Landstr. 1
D-85764 Neuherberg, Germany
Email: hrabe@helmholtz-muenchen.de

Abstract

G-protein-coupled receptors (GPCRs) represent targets for improved low-side-effect therapies to tackle the evolving Western obesity epidemic. The orphan (o) GPCR GPR101 emerged as an attractive candidate in this regard. Expressed on cells in brain areas regulating energy homeostasis, including the hunger-suppressing proopiomelanocortin (POMC) + neurons, it is minimally expressed outside the brain. To understand the function of this receptor *in vivo*, we herein generated and comprehensively characterized a *Gpr101* knockout mouse line, either under standard feeding conditions or with chronic high-fat diet (HFD) access (16 weeks). GPR101 loss accelerated the risk for diet-induced obesity (DIO), hyperinsulinemia and disrupted glucose homeostasis. Hypothalamic transcriptomic analysis revealed also decreased *Pomc* activation with HFD suggesting impaired hunger suppression. Moreover, on a standard diet, there was a molecular signature of downregulated tristetraprolin (TTP) pathway gene activation suggesting impaired inflammation resolution and one of aberrant microglial phagocytosis and lipid metabolism on HFD. Morphometry revealed altered hypothalamic arcuate nucleus microglial morphology consistent with the transcriptomic profile. We discuss how the GPR101 specialized pro-resolving mediator (SPM) receptor capacity likely underlies the aberrant microglial function and contributes to DIO risk. Thus, this evidence shows that GPR101 is a potential therapeutic target for DIO through, among other factors, effects on hypothalamic inflammation resolution.

Keywords: GPR101, Diet-induced obesity, insulin resistance, hypothalamus, inflammation

1. Introduction

According to the World Health Organisation (WHO), obesity prevalence numbers in Western society have almost tripled in the last 40 years. This is paralleled by increases in obesity-associated metabolic disorders including Type II diabetes (T2D), cardiovascular disease and non-alcoholic fatty liver disease (NAFLD) further impacting patient life quality and increasing mortality rates (Gregg et al. 2019; Saeedi et al. 2019). In certain cases, successful weight reduction and T2D treatment necessitate pharmacological intervention and so there is the need to develop more safe and efficacious therapies. In this regard, 'orphan' G-protein coupled receptors (oGPCRs), part of the seven transmembrane-spanning domain receptor family, localized to brain areas controlling feeding and energy balance regulation, provide novel and attractive therapeutic targets. While there is progress in GPCR deorphanization, the ongoing challenge lies in establishing the endogenous ligand(s) and function of these orphan receptors to determine their likely efficacy and potential side-effect profile (Ngo et al. 2016).

The class A oGPCR, GPR101, is of interest in this context. This receptor couples to Gs, Gαq/11, and Gα12/13 and strongly activates cAMP (Abboud et al. 2020). It is highly expressed in the brain, specifically in regions that control metabolism, reward and emotionality including the amygdala, nucleus accumbens and the arcuate nucleus (ARC) of the hypothalamus (Bates et al. 2006; Lee et al. 2001; Trivellin et al. 2016). Within these regions, GPR101 is expressed in ~55% of the anorexigenic proopiomelanocortin (POMC)+ neurons in ARC, glutamatergic neurons and thyrotropin-releasing hormone (TRH)+ neurons in the lateral hypothalamus and in a subset of γ-aminobutyric acid (GABA)+ and dopaminergic neurons in the ventral tegmental area (VTA) and substantia nigra (SN) (Nilaweera et al. 2007; Paul et al. 2019). While the physiology, function and known ligands of GPR101 remain largely unexplored, expression in different brain regions alters after energetic challenges e.g. food deprivation and during

lactation (Nilaweera et al. 2007; Nilaweera et al. 2008). This suggests an important role for GPR101 in energy homeostasis, a possibility supported by evidence of a SNP in the *GPR101* coding sequence associated with increased BMI in the Japanese population (missense variant (rs1190736 (C > A);p.Val124Leu)) (Akiyama et al. 2017). The developing pituitary gland also expresses GPR101. In humans, a pediatric disorder, X-linked acrogigantism (X-LAG), results from an Xq26.3 genomic duplication involving *GPR101,* characterized by early-onset gigantism due to hypersecretion of growth hormone (GH) (Trivellin et al. 2014). Moreover, in mice, overexpression of *Gpr101* under the control of the rat *Ghrhr* (growth hormone releasing hormone receptor) promoter (expressed in anterior pituitary somatotrophic cells) leads to chronic GH hypersecretion. Lower fat mass (with decreased adipocyte fat content and area) and hepatomegaly (with reduced liver fat) manifest in these transgenic mice (Abboud et al. 2020). Altogether, this evidence highlights the untapped potential of GPR101 as a therapeutic target for treating obesity.

In addition to roles in controlling body weight and GH secretion, GPR101 is the receptor mediating the leukocyte-directed actions of N-3 docosapentaenoic acid-derived resolvin D5 (RvD5n-3 DPA) in inflammatory arthritis (Flak et al. 2020). So-called specialized pro-resolving mediators (SPMs) resolve inflammation to restore homeostasis and include resolvins as well as lipoxins and protectins. As metabolic inflammation (metaflammation) may be involved in insulin resistance, curtailing inflammation could be beneficial for obesity and T2D (Charles-Messance et al. 2020). Thus, that RvD5n-3 DPA is a GPR101 agonist highlights an additional route through which targeting this receptor could benefit these disorders.

To understand the function of GPR101, we generated a GPR101 knockout (KO) mouse and assessed the metabolic phenotype on chow (CD) or chronic high-fat diet (HFD) feeding. As POMC is the precursor of adrenocorticotrophic hormone (ACTH), active in the hypothalamic-

pituitary-adrenal stress axis (Herman et al. 2016), we determined also the effect of GPR101 loss on mild stress responsivity. Mechanistically, we explored the effect of GPR101 deletion on hypothalamic gene expression and microglia and astrocyte numbers. The results from the study indicate augmented DIO and insulin resistance risk as well as altered POMC and inflammatory activation associated with GPR101 loss highlighting the potential of this receptor as a novel therapeutic target for appetite control and obesity.

2. Methods

2.1 Generation of GPR101 KO mouse

The C57BL/6NTac-*Gpr101*^{em7036Tac} mouse line with a constitutive Knock-Out (KO) of the *Gpr101* gene was custom-engineered using CRISPR/Cas9-mediated genome editing by Taconic Biosciences (https://www.taconic.com/genetically-engineered-animal-models/knockout-mice/). The NCBI transcript NM_001033360.3 formed the foundation for the targeting strategy. Deletion of exons 1 and 2 including approx. 1.5 kb of the promoter region resulted in the loss of function of the *Gpr101* gene by deleting the complete gene. We backcrossed the mouse line onto C57BL/6NTac and confirmed that GPR101 mRNA significantly decreased in our transcriptomic analysis of the hypothalamus of *Gpr101* KO mice (**Fig. 1A**). Mice were group-housed in individually ventilated cages (Kallnik et al. 2007) with water and standard mouse chow available *ad libitum* before the start of the experiment according to the directive 2010/63/EU. The care and use of animals and assays used in this study were approved and carried out according to the ARRIVE guidelines and the rules outlined by the ethical committees of the district government of Upper Bavaria (Regierung von Oberbayern) and the Helmholtz Zentrum München in Germany.

2.2 Experimental design and body weight analysis

All mice had access to standard chow up to the age of 7 weeks. At this time point, male mice were randomly selected from the wild-type littermate control ("WT") and the hemizygous *Gpr101* KO ("MUT") groups and were given access to 60% kcal from fat HFD (Research Diets, Inc.) until the end of the experiment. **Fig. 1B** depicts the experimental design used for this analysis. From the age of 11-23 weeks, all mice were phenotyped systematically in the German Mouse Clinic as described previously (Fuchs et al. 2018; Fuchs et al. 2009) and **Supplementary Fig. S1** shows the pipeline. The testing details described here are for those assays where there were genotype-pertinent alterations. We compared male MUT and WT mice on either standard chow (CD) or HFD and **Supplementary Table 1** shows the number of animals per group and age of testing for the different assays**.** The mice were weighed throughout the experimental timeline to determine their body weight evolution.

2.3 Open field

The 20-minute Open Field (OF) test was carried out at 11 weeks of age using the ActiMot system (TSE, Germany) as described previously (Garrett et al. 2012; Holter et al. 2015). The arena was made of transparent and infra-red light-permeable acrylic with a smooth floor (internal measurements: 45.5 x 45.5 x 39.5 cm, illumination = 150 lux corners, 200 lux middle).

2.4 Indirect calorimetry in metabolic homecages (MHC)

At the age of 15 weeks, MHC locomotor activity (distance travelled) and exploration (rearing), gas exchange (oxygen consumption and carbon dioxide production, VCO2/VO2), energy expenditure (heat production, kJ/h/animal), food intake and substrate utilisation of single-caged mice was measured by indirect calorimetry in metabolic home-cages (TSE, Germany, see:https://www.mousephenotype.org/impress/ProcedureInfo?action=list&procID=855&pip

eID=14). The measurement commenced five hours before lights off and finished four hours after lights-on the next morning (21 hours in total).

2.5 Body composition (qNMR lean/fat)

Our whole body composition analyzer (Bruker MiniSpec LF 50) based on Time Domain Nuclear Magnetic Resonance (TD-NMR) provides a robust method for the measurement of lean tissue and body fat in live mice without anaesthesia. It uses TD-NMR signals from all protons in the entire sample volume and provides data on lean and fat mass.

2.6 Glucose tolerance test (GTT)

Glucose metabolism disturbance was determined using the (GTT) at the age of 16 weeks. Glucose was administered intraperitoneally (2 g/kg i.p.) after a 16-h food withdrawal and basal fasting glucose levels and 15, 30, 60, and 120 minutes after glucose injection were measured from a drop of blood collected from the tail vein with the Accu-Chek Aviva Connect glucose analyzer (Roche/Mannheim).

2.7 Blood collection, hematology and immunology

The final blood samples were collected under isoflurane anaesthesia by retrobulbar puncture in Li-heparin-coated tubes. They were then stored on ice until centrifugation (4500xg, 10 Min) and separation of plasma aliquots for further analyses. The clinical chemistry analyses of circulating biochemical parameters in *ad libitum* fed mouse blood was performed using a clinical chemistry analyser (Beckman Coulter AU 480 autoanalyzer, Krefeld, Germany) at the age of 16 weeks. A broad set of parameters was measured including enzyme activities as well

as plasma concentrations of specific substrates and electrolytes (Rathkolb et al. 2013a; Rathkolb et al. 2013b).

2.8 Pathological examination

For pathological analyses at 16 weeks of age, hematoxylin and eosin (H&E) staining was performed on formalin-fixed paraffin-embedded sections (4 µm) from 28 organs. Two independent pathologists analysed the slides according to standardized protocols as previously described (Fuchs et al. 2018).

2.9 RNA isolation and transcriptome analysis of hypothalamus

Hypothalami were dissected and total RNA was isolated using the RNeasy Mini kit (Qiagen) including Trizol treatment. The Agilent 2100 Bioanalyzer was used to assess RNA quality and RNA with RIN > 7 was used for RNAseq analysis. Total RNA was analysed by RNA sequencing. Paired-end data was generated and analysed by a RNAseq pipeline consisting of quality control (FastQC, MultiQC), read trimming (trim_galore), genome alignment (STAR), and gene-level read counting (summarizeOverlaps, mode = 'Union'). The significantly regulated genes were determined with DEseq2 after excluding low expressed genes. For the biological interpretation of the observed gene regulation we performed protein-protein interaction analysis using the STRING database, Version 11.5 (www.string-db.org)(Szklarczyk et al. 2019), enrichment analyses with QIAGEN's Ingenuity Pathway Analysis software (IPA®, QIAGEN Redwood City, www.qiagen.com/ingenuity), and Enrichr (https://maayanlab.cloud/Enrichr/(Chen et al. 2013)). A more microglia-specific enrichment analysis was also performed using MGEnrichment (https://ciernialab.shinyapps.io/MGEnrichmentApp/). We used genome-wide transcriptome

analysis on 17 KO animals (9 HFD, 8 CD) and 15 WT animals (8 HFD, 7 CD). All samples passed the quality control criteria and we conducted statistical analyses with DEseq2.

2.10 Tissue collection, immunostaining and design-based stereological analysis of microglia and astrocyte populations

Adult mice were euthanised and perfused by transcardial perfusion with a solution of 4 % paraformaldehyde (PFA) in 0.1 M PBS (pH= 7.4). Dissected brains were post-fixed in the same fixative over night at 4 °C. Brains were transferred to a 30 % (w/v) sucrose solution and stored at 4 °C. 40 µm thick coronal sections were taken using a cryostat (Leica CM3050S), collected in cryoprotective solution (25 % ethylene glycol and 25 % glycerin in phosphate buffer) and stored at -20 °C. A one-in-six series of sections was used for each analysis.

For immunostaining of ionized calcium-binding adapter molecule 1 (IBA1)+ microglia and glial fibrillary acidic protein (GFAP)+ astrocytes, an Avidin-Biotin Complex (ABC) method like that employed previously (Garrett et al. 2020; Garrett et al. 2018; Ung et al. 2021) was used. For IBA1 immunostaining, the antibodies used were a primary goat monoclonal anti-Iba1 antibody (Abcam plc, Cambridge, UK; order no ab5076; dilution 1:200) with a biotinylated rabbit anti-goat IgG (1:300 Biotin-SP AffiniPure Rabbit Anti-Goat IgG, Jackson ImmunoResearch Inc., USA). For GFAP immunostaining, a primary rabbit monoclonal anti-GFAP antibody (Abcam plc, Cambridge, UK; order no ab4648; dilution 1:5000) was implemented in conjunction with a biotinylated goat anti-rabbit IgG (1:300 Biotin-SP AffiniPure Goat Anti-Rabbit IgG, Jackson ImmunoResearch Inc., USA). The tertiary ABC complex was employed according to manufacturer's instructions (VECTASTAIN Elite ABC HRP Kit PK-6100, VECTOR LABORATORIES, INC., Burlingame, USA). The negative controls, with omission of the primary antibodies, revealed no positive staining.

IBA1+ and GFAP+ cell numbers were estimated throughout the rostro-caudal extent of the hypothalamic ARC with design-based stereology using the StereoInvestigator software system (StereoInvestigator, MBF Biosciences Inc.). We also measured the cell density as the number of cells per size-matched counting frame. The estimates were made in every sixth serial 40-µm coronal section with the Optical Fractionator probe as described previously (Heermann et al. 2019). The observer was blind to the experimental groups. Two animals from each analysis were excluded due to tissue damaged during processing.

2.11 Microglial morphometric analysis

The branching morphology of the IBA1+ microglia was carried out as described previously (Ung et al. 2021) using a Zeiss Axio Imager M2 microscope (Carl Zeiss, Oberkochen, Germany) with a motorized stage and a CCD color camera and Neurolucida software (Version 2018) and Neurolucida Explorer (2018, MBF biosciences, Williston, VT, USA). Using the 100x objective, 5 microglial cells per animal were traced in the ARC between Bregma -1.22 - -2.54. Cell bodies of each cell were contoured in the Neurolucida program at the z-stage-level where it showed the biggest area in focus. The branches where traced in 3D focusing through the z-plane adjusting for branch thickness. The traced 3D-cell structures were analyzed in Neurolucida Explorer using the Branched Structure Analysis function. The parameters measured for each microglial cell were number of endings, branch length and volume. The coefficient of variation within the morphological parameters for each animal was lower than 0.5.

2.12 Statistics

Data was analysed using either 2-way ANOVA with genotype and diet as main factors or with separate t-tests to determine genotype differences on CD or HFD. A *post-hoc* Fisher's LSD was used to test genotype x diet interaction effects. A Grubb's test was used to identify outliers

that were subsequently excluded from the analysis (1 WT on CD and 1 WT on HFD for insulin levels, 1 MUT on HFD for TNF removed). For body weight evolution, body weight change and ipGTT analysis, a repeated measures (RM) ANOVA (with post-hoc Sidak's test) was implemented with time and genotype/diet as independent variables. Data was statistically analysed using GraphPad Prism version 8 for Windows (GraphPad Software, La Jolla, California, USA, www.graphpad.com). For all tests, a p value < 0.05 was the level of significance and data are mean ± SD. A correction for multiple testing was not performed.

2.13 Data availability

The RNA-seq data has been submitted to the GEO database at NCBI (GSE220533) and all phenotyping data will be available on the Phenomap Viewer of the German Mouse Clinic webpage (http://tools.mouseclinic.de/phenomap/jsp/annotation/public/phenomap.jsf).

3. Results

3.1 GPR101 loss increases vulnerability to DIO

To determine whether constitutive loss of GPR101 (**Fig. 1A** shows downregulation of hypothalamic *Gpr101*) would increase vulnerability to DIO, we gave *Gpr101* young adult male hemizygous KO and control mice *ad libitum* access to 60 % kcal from fat HFD over a period of 15-16 weeks from 7 weeks of age (**Fig. 1B**). Body weight measurements conducted over this period revealed that while a small increase in body weight was evident in the CD-fed MUT group, HFD consumption induced a more pronounced genotype difference as shown by the body weight evolution over time (**Fig. 1C**). This increased body weight was significant in the HFD-fed *Gpr101* mutant mice compared to controls during the first six weeks of HFD access (age 8 – 14 weeks). Nevertheless, there was higher within-group variation after this point and genotypic differences in absolute body weight diminished. This was reflected in the body

weight change where the mutant mice initially gained significantly more weight compared to controls however the magnitude of this difference was not as pronounced from week 6 onwards (**Fig. 1D**). We observed a significant reduction in food intake in the mutant group after 8 weeks on HFD (15 weeks of age) not evident on CD (**Fig. 1E**). In particular, 5/15 mutant mice (compared to 1/15 control mice) did not consume HFD.

Using non-invasive quantitative nuclear magnetic resonance, we determined the body composition of fat and lean content (aged 15 weeks, 8 weeks HFD). While there were no genotype differences in fat or lean mass on CD (**Fig. 1F**), HFD increased the mutant fat mass without altering lean mass (**Fig. 1G**) and increased the adiposity index (fat mass/lean mass, **Fig. 1H**). Furthermore, in spite of GPR101 overexpression association with acromegaly, we did not detect anatomical alterations in *Gpr101* KO mice compared to control mice after physical examination. There were also no significant genotypic differences in mean tibia length (**Fig. 1I**).

As GPR101 is highly expressed in the hypothalamic sub-nuclei and POMC+ neurons that also mediate stress reactivity (e.g. paraventricular nucleus of the HPA axis), we also determined the GPR101-loss effects on emotion-related behavior. There was slightly decreased anxiety-related behavior in mutant mice on CD in the open field (center entries increased, tendency to increased center time and distance), consistent with an existing *Gpr101* KO model (**Supplementary Fig. S2** for comparison). This anxiolytic effect is no longer evident on HFD. The corresponding basic neurological and locomotor functions assessed by SHIRPA, grip strength and rotarod were not affected by the mutation (All data will be available at http://tools.mouseclinic.de/phenomap/jsp/annotation/public/phenomap.jsf).

3.2 GPR101 ablation causes hyperinsulinemia

To assess the effect of GPR101 loss on the glycemic index we measured circulating insulin, fasted glucose levels and glucose tolerance. Insulin resistance occurs when there is an impairment of insulin ability to influence glucose metabolism requiring hyperinsulinemia to maintain signaling levels due to receptor downregulation and impaired glucose transport (Barazzoni et al. 2018). The *Gpr101* KO mice showed hyperinsulinemia compared to controls on both CD and HFD (**Fig. 2A**). To determine the association between this altered insulin state and effects on glucose regulation, we measured fasting glucose (after 6 weeks HFD) and performed the glucose tolerance test (ipGTT) after 10 weeks on HFD at 16 weeks of age. The loss of GPR101 slightly delayed glucose clearance on CD without differences on HFD (**Fig. 2B**) and did not alter circulating fasted glucose (**Fig. 2C**).

Reduced responsiveness to circulating insulin typifies insulin resistance and is a common feature of obesity that increases the risk of several pathological conditions, including hyperinsulinemia, glucose intolerance, T2D, cardiovascular disease and NAFLD. Liver weight (body weight normalized), measured at the end of the study, tended to increase with GPR101 loss and HFD feeding and qualitative analysis of H&E stained liver sections suggests an exacerbation of HFD-induced lipid accumulation with GPR101 loss (**Fig.2D, E**). Increased weight with lipid accumulation in the liver increases NAFLD risk.

3.3 GPR101 loss alters hypothalamic immuno-regulatory gene expression

Given the hypothalamic GPR101 expression and that HFD-induced gliosis and metabolic stress lead to hypothalamic circuit dysfunction (De Souza et al. 2005; Kothari et al. 2017), we performed RNA-Seq analysis of this region to investigate the molecular basis for the GPR101 loss-associated increased DIO risk (in 21-week-old mice, 15 weeks HFD, full gene lists and

summary of all analyses in **Supplementary information gene lists, Tables 2-6**). We observed 227 differentially expressed genes (DEGs) in mutant mice compared to controls on HFD and 179 on CD (with raw $P < 0.01$, not significant with *P*adj). To understand the functional significance of the DEGs, we used the STRING ('Search Tool for Retrieval of Interacting Genes/Proteins') database, to determine the predicted interactions of the genes upregulated or downregulated in the *Gpr101* KO mice under CD or HFD conditions. We also enlisted the Enrichr and MGEnrichment databases for enrichment analysis. This method entails the systematic association of the genesets with biological terms to derive a mechanistic impression. While it will reveal whether DEG subsets are relevant to a particular function or disease, further experimental validation is necessary to understand how up- or down-regulation of specific genes affect the ascribed function. We describe below the main outcome for each dietary condition separately, focusing on the most strongly significant DEGs and those forming protein interaction networks (the full list of DEGs can be found in the **Supplementary information**).

DEGs in mutant mice on CD: Under standard CD conditions, among other genes, GPR101 loss caused upregulation of the disease-associated microglia (DAM) gene *Trem2* (Triggering receptor expressed on myeloid cells 2) (**Fig. 3A, upper panel**). TREM2 is expressed predominantly in microglia in the brain, playing an immune homeostatic role, necessary for microglial proliferation, migration, phagocytosis, cytokine release, lipid sensing and ApoE binding(Atagi et al. 2015; Kleinberger et al. 2014; Ulrich and Holtzman 2016). Upregulation of hypothalamic TREM2 with GPR101 loss under standard conditions suggests potential immune activation. Accordingly, this was accompanied by downregulation of the gene encoding ZFP36 (Zinc-finger protein 36 or Tristetraprolin (TTP)) and the related protein functional interaction network (**Fig. 3A, lower panel**, *Zfp36, Btg2, Dusp1, Nr4a1, Egr1, Fosb, Klf4, Klf2, Atf3* and *Ier2*,

Table 1 for functional annotations). TTP is an RNA-binding protein controlling RNA stability and is anti-inflammatory by guiding unstable pro-inflammatory protein mRNA. TTP loss thereby has the potential to elevate TNF-α cytokine expression and enhance hypothalamic inflammation through activating microglia (as is evidenced here by *Trem2* upregulation) altering energy expenditure (Jeong et al. 2021).

The enrichment analysis of *Gpr101* KO mouse DEGs on CD revealed a significant overrepresentation of genes associated with "*TNF alpha Signaling by NF-kB"* and "*Astrocyte:Brain"* (for downregulated DEGs), microglia (for both up- and down-regulated genes), and "*Oligodendrocyte Brain Non-Microglia"* (for upregulated DEGs) encompassing the ZFP36 network/TTP genes and *Trem2* (**Fig. 3B,** see **Supplementary Information** for full enrichment terms and analysis details). In this case, that the enriched term "*TNF-alpha Signaling by NF-kB"* concerns the TTP interactome DEGs (see **Supplementary Information** for the list of genes associated with each enriched term) is consistent with the afore mentioned TNF-α activating effects of TTP impairment. Overall, this pattern indicates a state of altered immuno-regulation and microglial activity as a result of GPR101 loss under standard feeding conditions. Given this profile, we performed an additional microglia (MG)-specific functional enrichment analysis of this gene set using the MGEnrichment tool (Jao and Ciernia 2021) (**Fig. 3C**, full details and term explanations in **Supplementary information**). On CD, among other MG-terms, the mutant mouse hypothalamic DEGs were significantly enriched for: "*DAMstage1 < DAMstage2 MG*" (for up- and down-regulated genes) and "*Microglia anti-inflammatory responses*" (for downregulated genes). Collectively, this infers that loss of GPR101 on CD induces a hypothalamic molecular signature (of both up- and down-regulated DEGs) characteristic of stage 2 DAMs (rather than stage 1) and altered microglial anti-inflammatory responsivity. DAMs are produced through a two-step mechanism (Keren-Shaul

et al. 2017) transitioning from the resting/homeostatic microglial state to an intermediate (stage 1) and then to a TREM2-dependent activation state (stage 2). This evolution includes upregulation of *Trem2* and downregulation of the anti-inflammatory TTP interactome genes, consistent with the hypothalamic pattern observed with GPR101 loss under standard conditions.

DEGs in mutant mice on HFD: On HFD, we found upregulation of genes involved in excitatory and inhibitory neurotransmission *(Gabra3* [GABAergic receptor subunit alpha-3 gene], *Lrrtm2* [Leucine-rich repeat transmembrane neuronal protein-2]) as well as appetite control (*Ankrd26* [Ankyrin repeat domain 26]) (**Fig. 3D, upper panel**). Furthermore, the ciliogenesis genes *Ttbk2* (Tau-tubulin kinase 2) and *Ccp110* (Centriolar coiled-coil protein of 110 kDa) were upregulated, that directly and indirectly (via *Ttbk2*) interact with *Ankrd26*. The encoded ANKRD26 protein regulates adipogenesis and KO in mice caused hyperphagia and obesity (Acs et al. 2015). In parallel, the *Gpr101* KO mice on HFD showed downregulation of the anorexigenic *Pomc* gene, inflammation and microglia-related genes (*Rela*, *Csf1r, C1qc, Hcls1, Masp1, Ubc, Ripk1, Tifa*), endothelial cell signaling and integrity-related genes (*Vegf3* (*Figf*), Vegfr-3 (*Flt4*), *Emcn, Ramp2, Ramp1, Timp4, Mmp14*), phagocytosis-related genes (*Gabarap, Cyba*), as well as lipid metabolism and lipoprotein signaling-related genes (*Lrp10, Lipg, Acsbg1*) (**Fig. 3D, lower panel**). *Lrp10* (low-density lipoprotein receptor-related protein 10) mediates internalization of lipophilic ApoE implicated in cholesterol efflux and microglial phagocytosis(Gibbons et al. 2010),(Jeong et al. 2019). The *Acsbg1* (Acyl-coa synthetase bubblegum family member 1) gene encodes a protein that activates cellular lipid synthesis and degradation. *Lipg* encodes an endothelial lipase with phospholipase and triglyceride lipase activity. Impaired autophagy, as indicated by downregulated *Gabarap* and *Cyba*, can lead to changes in lipid metabolism (Saito et al. 2019).

Within the mutant DEGs on HFD, there was enrichment of the terms "*BDNF regulation of GABA"* (for upregulated DEGs), *"TNFR2 signaling", "Matrix Metalloproteinase inhibition"* and *"Endothelial cell"* (for downregulated DEGs, **Fig. 3E**). With the MGEnrichment tool, we found enrichment of the terms "*DAMstage1 < DAMstage2 MG*" for upregulated and "*Amoeboid>Ramified MG*" and "*DAM<HOM MG*" for downregulated mutant DEGs (**Fig. 3F**). This suggests that GPR101 loss on HFD produces a molecular signature consistent with stage 2 DAM activation (with less homeostatic ("*DAM<HOM MG*") microglial gene expression) yet with more ramified compared to amoeboid microglial morphology indicative of a less phagocytic state. Overall, this transcriptomic evidence indicates that loss of GPR101 leads to blunted hypothalamic microglial phagocytosis, impaired lipid metabolism and aberrant endothelial cell signaling and integrity after 15 weeks on HFD. Neither *Gh* nor its receptors were differentially regulated in the hypothalamus with GPR101 loss (**Supplementary Fig. S6**).

3.4 GPR101 loss alters immune markers and hypothalamic microglial morphology

Based on the transcriptomic analysis, we performed a more detailed investigation of inflammatory markers as well as microglia and astrocyte cell populations in the ARC of the hypothalamus. Pro-inflammatory activation of macrophages is causally linked to obesity and obesity-associated disorders, e.g. systemic insulin resistance and NAFLD due to chronic activation of stress- and inflammation-related kinases. GPR101 loss on HFD feeding induced innate immune response activation that was not evident with intact functioning of this protein on the same diet. This was manifest as increased circulating monocyte ((**Fig. 4A, left panel**) and TNF-α (**Fig. 4A, right panel**) levels in the mutant mice.

We used design-based stereology to quantify microglial (IBA1+) and astrocyte (GFAP+) cell density and microglial morphometry to index microglial activation. Our analysis revealed that

astrocyte density increased on HFD with no apparent influence of GPR101 loss (**Fig. 4B, right panel**). Furthermore, while HFD did not significantly alter microglia density at this time point (23 weeks of age, 16 weeks HFD), loss of GPR101 function increased microglia density in the ARC (**Fig. 4C, right panel**). As described, the MGEnrichment analysis revealed GPR101 loss caused differential regulation of genes affecting amoeboid microglial morphology formation. When activated, the microglial cell soma is enlarged and less ramified with shorter branches yielding an amoeboid appearance, emblematic of ongoing phagocytosis(Morrison and Filosa 2013). Previous evidence shows that hypothalamic ARC microglia increase in size with 16 weeks HFD (Valdearcos et al. 2014). Nevertheless, GPR101 deficient mice exhibited more elongated ramified ARC microglia on HFD compared to CD (**Fig. 4D**), with increased branch number ("Ends", **Fig. 4E left panel**), volume (**Fig. 4E, middle panel**) and branch length (**Fig. 4E right panel**). The latter tended to be increased compared to WT on HFD and this pattern was not evident in mice with functioning GPR101 (**Fig. 4E right panel**). Overall, the morphology indicates that GPR101 deficient microglia are enlarged and exhibit impaired phagocytosis in response to HFD.

4. Discussion

The oGPCR GPR101 is a promising target for metabolic disease treatment due to expression in brain regions controlling energy homeostasis (Bates et al. 2006; Nilaweera et al. 2007). To elucidate further the function and role of this receptor in energy balance regulation, we scrutinized a *Gpr101* full knockout mouse line (hemizygous males) under both standard and chronic HFD feeding conditions. Building on extant correlational mouse (Nilaweera et al. 2007) and human data (Akiyama et al. 2017), we showed that *Gpr101* loss heightened DIO risk during HFD challenge with a persistent body composition shift to increased adiposity. Moreover, there was genotype-dependent hyperinsulinemia (with and without HFD) and reduced glucose tolerance (on CD), hinting towards increased insulin resistance in mutants. Our hypothalamic transcriptomic analysis indicated that constitutive loss of GPR101 alters feeding, lipid metabolism, microglial and inflammation-associated gene activation both under balanced and HFD conditions. This was coupled with aberrant surrogate indices of hypothalamic microglial activity that likely, among other factors, contributed to the heightened DIO risk. Consonant with the pleiotropy and ability of GPCRs to respond to multiple ligands, there are potentially several underlying factors involved (discussed below) (Wacker et al. 2017).

Direct effects of GPR101 loss on the hypothalamic neurons mediating feeding and energy homeostasis can contribute to the associated DIO risk. Existing correlational data implicates GPR101 in appetite and feeding regulation (Nilaweera et al. 2007). Expressed in a subset of anorexigenic POMC+ (~55%) and orexigenic NPY+ (5%) neurons (Nilaweera et al. 2007), activation putatively facilitates the release of the melanocortins α-, β- and γ-melanocyte stimulating hormone (MSH) suppressing appetite (Bagnol 2010). That GPR101 ablation decreased hypothalamic *Pomc* activation on HFD likely undermined this response promoting

hunger and feeding. While it is not apparent why GPR101 loss then reduced food intake at 8 weeks on HFD, an initial increased HFD feeding may be blunted over time by parallel alterations suggested by the hypothalamic transcriptomic profile. For example, the GABAergic receptor subunit *Gabra3* and the glutamatergic AMPA receptor-anchoring *Lrrtm2* were both upregulated in the mutant hypothalamus on HFD indicating changes in inhibitory and excitatory function. It is thus relevant, for example, that in the POMC/GABAergic neuron subset, *Pomc* expression restores normal food intake in obese mice (Trotta et al. 2020). Given the diversity of POMC+ cell subpopulations, analysis of POMC+ cell specific *Gpr101* knockout mice will aid in understanding the function in these cells (Steuernagel et al. 2022). In addition *Ankrd26* along with associated ciliogenesis genes *Ttbk2* and *Ccp110* upregulated with GPR101 KO on HFD. The ANKRD26 protein regulates adipogenesis and disruption in mice caused obesity, insulin resistance and increased feeding behaviour putatively through primary ciliopathy of the melanocortin pathway neurons (Acs et al. 2015; Bera et al. 2008). Increased ANKRD26 activation with primary ciliogenesis therefore potentially offsets the effects of GPR101 loss on feeding and metabolic regulation for confirmation in future studies. Altered GH signalling due to GPR101 loss may also contribute to fat accumulation and hyperinsulinemia (Sharma et al. 2018) (Abboud et al. 2020; Rodd et al. 2016; Sharma et al. 2018). Nevertheless, the tibia length did not differ to suggest altered developmental growth nor were *Gh* related transcripts differentially expressed in the hypothalamic transcriptome. Thus, confirmation of both altered pulsatile GH release and regulation would be propitious.

Our analysis revealed further mechanistic insights into the DIO-susceptibility associated with GPR101 loss. Under both dietary conditions, the mutant transcriptomic profile indicated altered hypothalamic inflammatory signalling, microglia, endothelial cell and lipid metabolism-related gene activation. Disrupted TTP activity with GPR101 ablation on CD can

produce a chronic inflammatory state seen also in inflammatory arthritis (Ross et al. 2017). This finding of apparent impaired inflammation resolution tallies with the established GPR101 pro-resolving function as the SPM RvD5n-3 receptor (Flak et al. 2020). In addition, obstructed TTP associates with activated microglia, a possibility supported by upregulated *Trem2* in CD-fed *Gpr101* KO mice. TREM2 is a lipid-sensitive marker of DAMs that stimulates phagocytosis (Boche and Gordon 2022). In general, hypothalamic microglia sense and initiate inflammatory and phagocytic reactions to dietary excess before metabolic adaptations; a process obstructed in obesity (Mendes et al. 2018). Even without a dietary challenge, activated microglia, as inferred by the transcriptomic profile of *Gpr101* KO mice already on CD, promote weight gain and immune primed-microglia increase DIO susceptibility (Fernandez-Arjona et al. 2022; Valdearcos et al. 2017). After 15 weeks on HFD, the hypothalamic DEG profile in the mutant mice was one of impaired lipid sensing and metabolism and blunted microglial phagocytosis that may have also elevated the DIO risk and/or are responses to protracted nutritional challenge. Within the hypothalamus, microglia are necessary for lipid detection and debris clearance, the impairment of which contributes to their inflammatory activation and excess lipid accumulation (Folick et al. 2021). Thus, GPR101 loss could have accelerated DIO risk on HFD due to inappropriate microglial lipid sensing.

A new microglia classification was defined recently, the so-called 'lipid droplet accumulating microglia' (LDAM) (Marschallinger et al. 2020). These cells are typified by excessive lipid droplet intake, defective phagocytosis and high reactive oxygen species (ROS) and proinflammatory cytokine levels. TTP (ZFP36) pathway genes were among the top differentially expressed in LDAMs (Marschallinger et al. 2020). GPR101 dysfunction may induce LDAM generation as supported by the aberrant lipid metabolism transcriptomic profile. Moreover, the increased microglial end number, volume and branch length in the HFD-fed

mutant group infers LDAM-typical decreased phagocytosis (Kettenmann et al. 2011). As the RvD5 receptor in macrophages, GPR101 increases effero- and phago-cytosis (Flak et al. 2020). Microglia also express SPM receptors and can respond to resolvins in neuroinflammation resolution (Tiberi and Chiurchiu 2021). GPR101 loss likely then undermined the microglial pro-resolving capacity. The concomitant increased vulnerability to LDAM formation can fuel the HFD-induced inflammation, lipid accumulation, impaired phagocytosis, increased POMC+ cell loss and elevated DIO risk. A more in-depth scrutiny of GPR101 deficient microglia will shed more light on associated DIO risk.

4.1 Conclusion

To conclude, we have shown that constitutive GPR101 loss in male mice increases the risk for DIO and insulin resistance that may relate to the loss of hypothalamic satiety neurons and microglial pro-resolving inflammation function of this receptor. There is more investigation needed to identify the GPR101 ligand(s) that produce these pathogenic effects as well as the confirmation of the underlying physiological mechanisms. Nevertheless, these initial gene ablation phenotypes reinforce the therapeutic promise of this receptor for human obesity patients paving the way for additional research into GPR101.

Acknowledgments

We thank Ronan le Gleut (Helmholtz Zentrum München, ICB, Core Facility Statistical Consulting) for statistical advice as well as the technical staff from the German Mouse Clinic at Helmholtz Zentrum München. The study was supported by the German Federal Ministry of Education and Research (Infrafrontier grant 01KX1012 to MHdA); German Center for Diabetes Research (DZD) (MHdA).

Author contributions (names must be given as initials)

LG, MI, AB, BR, RG, LB, ASM, AAP, RR, YLC, MK, JCW, HF, VGD, SMH, TZ conceptualised the experiment, developed and executed the methodology, performed the formal analysis with statistics, conducted the research and analysed and interpreted the data, wrote the manuscript, reviewed and edited the manuscript. WW, MHdA, TZ and SMH reviewed and edited the manuscript, supervised and lead the research activity. MHdA and WW acquired the funding necessary to conduct the research.

Additional Information (including a Competing Interests Statement)

AB and TZ are employees of Boehringer Ingelheim Pharma GmbH & Co. KG. AB and TZ declare no competing financial interest in this work.

Figure Legends

Figure 1. Loss of *Gpr101* increased susceptibility to diet-induced obesity (DIO) on high-fat diet (HFD). Transcriptomic analysis of the hypothalamus revealed clear loss of *Gpr101* (**A**) in the mutant mice (MUT) compared to wildtype controls (WT) regardless of feeding with chow diet (CD) or HFD. ****p<0.0001 genotype effect in 2-way ANOVA. (**B**) The experimental design overview with the age at which the mice received HFD and the different assays performed (generated at www.biorender.com). WT and MUT mice consumed a 60 % kcal HFD from the age of 7 weeks with a WT and MUT group remaining on CD. While a small increase in body weight was evident in the CD-fed MUT group, HFD consumption induced a more pronounced genotype difference as shown by the body weight evolution over time (**C**). Body weight change during initial weeks on HFD compared to starting body weight was significantly higher in MUT mice compared to WT (**D**). The magnitude of this difference diminished from 6 weeks on HFD. The HFD-fed mice also decreased food intake compared to WT during indirect calorimetry

analysis at 15 weeks (**E**). Fat (**F**) and lean (**G**) mass were measured at the age of 15 weeks (8 weeks of HFD). HFD feeding significantly increased fat mass in the MUT mice without altering lean mass. The adiposity index of fat mass (FM) in ratio to lean mass (LM) was increased in HFD-fed MUTs (**H**). The tibia length was normal in the MUT mice (**I**). *p<0.05, **p<0.01, ****p<0.0001 WT vs. MUT.

Figure 2. Loss of *Gpr101* increased insulin resistance risk and impaired glucose clearance. Constitutive loss of *Gpr101* (MUT) caused increased circulating plasma insulin levels with high-fat diet (HFD) and without (CD – chow diet) compared to wildtype controls (WT) (**A**). In the intraperitoneal glucose tolerance test (ipGTT), used to assess glucose clearance after i.p. injection of a glucose bolus, there was slightly impaired glucose clearance in the MUT compared to WTs under CD conditions (**B**). The effect was not apparent with HFD. There were no differences between the genotypes in fasting glucose levels with either feeding condition (**C**). Liver weight tended to increase in MUT group with HFD and not with CD (**D**). The increased liver weight was associated with qualitative liver histological alterations indicative of increased fat deposition (**E**). **p < 0.01, MUT vs. WT

Figure 3. GPR101 loss induced aberrant hypothalamic expression of inflammation, microglial and feeding-related genes with and without high-fat diet challenge. Functional analysis of hypothalamic differentially expressed genes (DEGs) from *Gpr101* knockout ("MUT") and control ("WT") mice on either standard chow-diet (CD) or 60 % kcal high-fat diet (HFD) from 21-week old mice after 15 weeks HFD. (**A**) A STRING (Search Tool for the Retrieval of Interacting Genes/Proteins) predicted functional association network for upregulated (upper panel) and downregulated (lower panel) DEGs in mutant mice on CD with the main evidence for protein-protein interactions (PPIs) depicted. The legend (taken from string-db.org) is also shown. Each node is representative of all proteins produced by a protein coding gene. The

edges indicate protein-protein associations with shared functions. Magenta- and cyan-colored edges are established interactions and the remainder are predicted interactions. Upregulated genes (top panel) included *Trem2* (Triggering receptor expressed on myeloid cells 2) activated in disease associated microglia (DAM). For downregulated DEGs in mutant mice on CD (lower panel), there was a significant PPI network for the ZFP36/Tristetraprolin (TTP) protein (related nodes highlighted in purple), the downregulation of which is associated with increased inflammation. Depicted are selected significant terms from the enrichment analysis of the MUT DEGs on CD using the *Enrichr* platform accessing different databases (https://maayanlab.cloud/Enrichr/) (**B**) and with the microglia-specific MGEnrichment analysis tool (https://ciernialab.shinyapps.io/MGEnrichmentApp/) (**C**). In the STRING analysis of DEGs in MUT mice on HFD, there was upregulation (upper panel) of genes involved in glutamatergic (*Lrrtm2*) and GABAergic (*Gabra3*) signaling (**D**). *Ankrd26* and associated ciliogenesis genes (*Ttbk2, Ccp110*) were also upregulated in MUT mice on HFD. The anorexigenic *Pomc* was downregulated (lower panel) in MUT mice on HFD as were genes associated with inflammation and microglia (*Rela, Csf1r, C1qc, Hcls1, Masp1, Ubc, Ripk1, Tifa*), endothelial cell signaling and integrity (Vegfd (*Figf*), Vegfr3 (*Flt4*), *Emcn, Ramp2, Ramp1, Timp4, Mmp14*), phagocytosis (*Gabarap, Cyba*) and lipid metabolism (*Lrp10, Lipg, Acsbg1*). Selected significant enriched terms from the enrichment analysis with Enrichr (**E**) and (**F**) MGEnrichment for the upregulated and downregulated MUT DEGs on HFD. FDR = false discovery rate. The raw p values and significance are depicted in the respective bar. *p<0.05, **p<0.01, ***p <0.001.

Figure 4. GPR101 loss altered innate immune response markers and hypothalamic microglial morphology with high-fat diet (HFD) feeding. (A) Circulating monocytes were increased with HFD-fed *Gpr101* knockout (KO or “MUT”) mice compared to both HFD-fed wildtype (“WT” and

588 chow diet (CD)-fed MUT (Left panel). A similar pattern was evident for circulating tumor
589 necrosis factor (TNF)-alpha, the proinflammatory cytokine, produced by
590 monocytes/macrophages (Right panel). (**B**) Left and middle panels show representative
591 photomicrographs of the astrocyte marker, glial fibrillary acidic protein (GFAP), staining
592 patterns in WT CD and HFD fed mice. The cell density estimates (Right panel) revealed clearly
593 increased (GFAP)+ astrocyte cells with HFD consumption in the hypothalamic arcuate nucleus
594 (ARC) but this was not altered by *Gpr101* loss. (**C**) Left and middle panels show representative
595 photomicrographs of the Ionized calcium binding adaptor molecule 1 (IBA1)+ microglial
596 marker immunostaining from WT CD and HFD fed mice. The cell density estimates are shown
597 in the right panel and reveal increased density in the ARC of HFD-fed MUT mice compared to
598 CD-fed MUT mice. The WT mice did not show a similar increase. (**D, E**) The morphological
599 analysis of ARC IBA1+ microglia from mice of each group revealed that HFD caused increased
600 IBA1+ microglia volume, number of branch ends and branch length in MUT mice compared to
601 CD-fed MUT mice. The microglial branch length also tended to be higher in the HFD-fed MUT
602 compared to WT mice. Data comparisons with 2-way ANOVA with post-hoc LSD test. *p<0.05,
603 **p<0.01 WT vs. MUT, #p<0.05, ##p<0.01, ###p<0.001 CD vs. HFD. 3V = third ventricle. Scale
604 bar = 10 mm. Black arrows highlight immuno-stained cells (astrocytes or microglia)

605 **Table 1.** Protein annotations of hypothalamic differentially expressed genes with GPR101 loss
606 and high-fat diet feeding. From https://string-db.org

Gene	*Protein annotation*
Btg2	BTG2; Anti-proliferative protein; the function is mediated by association with deadenylase subunits of the CCR4-NOT complex. Activates mRNA deadenylation in a CNOT6 and CNOT7-dependent manner. In vitro can inhibit deadenylase activity of CNOT7 and CNOT8. Involved in cell cycle regulation. Could be involved in the growth arrest and differentiation of the neuronal precursors. Modulates transcription regulation mediated by ESR1. Involved in mitochondrial depolarization and neurite outgrowth (By similarity); Belongs to the BTG family (158 aa)
Ccl12	C-C motif chemokine 12; Chemotactic factor that attracts eosinophils, monocytes, and lymphocytes but not neutrophils. Potent monocyte active chemokine that signals through CCR2. Involved in allergic inflammation and the host response to pathogens and may play a pivotal role during early stages of allergic lung inflammation; Belongs to the intercrine beta (chemokine CC) family (104 aa)

Klf2	Kruppel-like factor 2 (lung); Krueppel-like factor 2; Transcription factor that binds to the CACCC box in the promoter of target genes such as HBB/beta globin or NOV and activates their transcription (354 aa)
Hist1h4j	H4 clustered histone 6; Histone cluster 1, H4j; Core component of nucleosome. Nucleosomes wrap and compact DNA into chromatin, limiting DNA accessibility to the cellular machineries which require DNA as a template. Histones thereby play a central role in transcription regulation, DNA repair, DNA replication and chromosomal stability. DNA accessibility is regulated via a complex set of post-translational modifications of histones, also called histone code, and nucleosome remodeling (103 aa)
Atf3	Cyclic AMP-dependent transcription factor ATF-3; This protein binds the cAMP response element (CRE) (consensus: 5'-GTGACGT[AC][AG]-3'), a sequence present in many viral and cellular promoters. Represses transcription from promoters with ATF sites. It may repress transcription by stabilizing the binding of inhibitory cofactors at the promoter (By similarity); Belongs to the bZIP family. ATF subfamily (181 aa)
Nr4a1	Nuclear receptor subfamily 4, group a, member 1; Nuclear receptor subfamily 4 group A member 1; Orphan nuclear receptor. May act concomitantly with NURR1 in regulating the expression of delayed-early genes during liver regeneration. Binds the NGFI-B response element (NBRE) 5'- AAAAGGTCA-3'. May inhibit NF-kappa-B transactivation of IL2. Participates in energy homeostasis by sequestrating the kinase STK11 in the nucleus, thereby attenuating cytoplasmic AMPK activation (By similarity) (601 aa)
Fseg	DEPP1 autophagy regulator; Protein DEPP1; Acts as a critical modulator of FOXO3-induced autophagy via increased cellular ROS (205 aa)
Klf4	Krueppel-like factor 4; Transcription factor; can act both as activator and as repressor. Binds the 5'-CACCC-3' core sequence. Binds to the promoter region of its own gene and can activate its own transcription. Regulates the expression of key transcription factors during embryonic development. Plays an important role in maintaining embryonic stem cells, and in preventing their differentiation. Required for establishing the barrier function of the skin and for postnatal maturation and maintenance of the ocular surface. Involved in the differentiation of epithelial cells and may also fu [...] (483 aa)
Cytip	Cytohesin-interacting protein; By its binding to cytohesin-1 (CYTH1), it modifies activation of ARFs by CYTH1 and its precise function may be to sequester CYTH1 in the cytoplasm (359 aa)
Gpr101	Probable G-protein coupled receptor 101; Orphan receptor (511 aa)
Ier2	Immediate early response gene 2 protein; DNA-binding protein that seems to act as a transcription factor (By similarity). Involved in the regulation of neuronal differentiation, acts upon JNK-signaling pathway activation and plays a role in neurite outgrowth in hippocampal cells (By similarity). May mediate with FIBP FGF-signaling in the establishment of laterality in the embryo (By similarity). Promotes cell motility, seems to stimulate tumor metastasis (By similarity) (221 aa)
Dusp1	Dual specificity protein phosphatase 1; Dual specificity phosphatase that dephosphorylates MAP kinase MAPK1/ERK2 on both 'Thr-183' and 'Tyr-185', regulating its activity during the meiotic cell cycle; Belongs to the protein-tyrosine phosphatase family. Non-receptor class dual specificity subfamily (367 aa)
C1qtnf3	Complement c1q tumor necrosis factor-related protein 3; C1q and tumor necrosis factor related protein 3 (319 aa)
Egr1	Early growth response protein 1; Transcriptional regulator. Recognizes and binds to the DNA sequence 5'-GCG(T/G)GGGCG-3'(EGR-site) in the promoter region of target genes. Binds double-stranded target DNA, irrespective of the cytosine methylation status (By similarity). Regulates the transcription of numerous target genes, and thereby plays an important role in regulating the response to growth factors, DNA damage, and ischemia. Plays a role in the regulation of cell survival, proliferation and cell death. Activates expression of p53/TP53 and TGFB1, and thereby helps prevent tumor forma [...] (533 aa)
Cdc20b	Cell division cycle 20B (519 aa)
Fosb	Fbj osteosarcoma oncogene b; Protein fosB; FosB interacts with Jun proteins enhancing their DNA binding activity; Belongs to the bZIP family. Fos subfamily (338 aa)
Scin	Adseverin; Ca(2+)-dependent actin filament-severing protein that has a regulatory function in exocytosis by affecting the organization of the microfilament network underneath the plasma membrane. Severing activity is inhibited by phosphatidylinositol 4,5-bis-phosphate (PIP2) (By similarity). In vitro, also has barbed end capping and nucleating activities in the presence of Ca(2+). Required for megakaryocyte differentiation, maturation, polyploidization and apoptosis with the release of platelet-like particles (By similarity). Plays a role in osteoclastogenesis (OCG) and actin cytoskele [...] (715 aa)
9530053A07Rik	RIKEN cDNA 9530053A07 gene (2581 aa)
Zfp36	mRNA decay activator protein ZFP36; Zinc-finger RNA-binding protein that destabilizes numerous cytoplasmic AU-rich element (ARE)-containing mRNA transcripts by promoting their poly(A) tail removal or deadenylation, and hence provide a mechanism for attenuating protein synthesis. Acts as an 3'-untranslated region (UTR) ARE mRNA-binding adapter protein to communicate signaling events to the mRNA decay machinery. Recruits deadenylase CNOT7 (and probably the CCR4-NOT complex) via association with CNOT1, and hence promotes ARE-mediated mRNA deadenylation. Functions also by recruiting compon [...] (319 aa)
Aipl1	Aryl-hydrocarbon-interacting protein-like 1; May be important in protein trafficking and/or protein folding and stabilization (328 aa)

E2f8	Transcription factor E2F8; Atypical E2F transcription factor that participates in various processes such as angiogenesis and polyploidization of specialized cells. Mainly acts as a transcription repressor that binds DNA independently of DP proteins and specifically recognizes the E2 recognition site 5'-TTTC[CG]CGC-3'. Directly represses transcription of classical E2F transcription factors such as E2F1: component of a feedback loop in S phase by repressing the expression of E2F1, thereby preventing p53/TP53-dependent apoptosis. Plays a key role in polyploidization of cells in placenta a [...] (860 aa)
Ssx9	MCG116991, isoform CRA_b; Synovial sarcoma, X breakpoint 9 (170 aa)
Apold1	Apolipoprotein L domain containing 1 (246 aa)
Ccna2	Cyclin-A2; Cyclin which controls both the G1/S and the G2/M transition phases of the cell cycle. Functions through the formation of specific serine/threonine kinase holoenzyme complexes with the cyclin-dependent protein kinases CDK1 and CDK2. The cyclin subunit confers the substrate specificity of these complexes and differentially interacts with and activates CDK1 and CDK2 throughout the cell cycle (422 aa)
Kri1	KRI1 homolog (S. cerevisiae); Belongs to the KRI1 family (705 aa)
D630003M21Rik	Uncharacterized protein KIAA1755 homolog; RIKEN cDNA D630003M21 gene (1187 aa)
Gpr101	Probable G-protein coupled receptor 101; Orphan receptor (511 aa)
Pgap1	Post-gpi attachment to proteins 1; GPI inositol-deacylase; Involved in inositol deacylation of GPI-anchored proteins. GPI inositol deacylation may important for efficient transport of GPI-anchored proteins from the endoplasmic reticulum to the Golgi (By similarity) (922 aa)
Dnm1l	Dynamin-1-like protein; Functions in mitochondrial and peroxisomal division. Mediates membrane fission through oligomerization into membrane- associated tubular structures that wrap around the scission site to constrict and sever the mitochondrial membrane through a GTP hydrolysis-dependent mechanism. Through its function in mitochondrial division, ensures the survival of at least some types of postmitotic neurons, including Purkinje cells, by suppressing oxidative damage. Required for normal brain development, including that of cerebellum. Facilitates developmentally regulated apoptos [...] (716 aa)
Acsbg1	Acyl-coa synthetase bubblegum family member 1; Long-chain-fatty-acid--CoA ligase ACSBG1; Mediates activation of long-chain fatty acids for both synthesis of cellular lipids, and degradation via beta-oxidation. Able to activate long-chain fatty acids. Can activate diverse saturated, monosaturated and polyunsaturated fatty acids (By similarity) (721 aa)
Elavl4	ELAV-like protein 4; May play a role in neuron-specific RNA processing. Protects CDKN1A mRNA from decay by binding to its 3'-UTR. Binds to AU-rich sequences (AREs) of target mRNAs, including VEGF and FOS mRNA (By similarity) (385 aa)
Pak3	Serine/threonine-protein kinase PAK 3; Serine/threonine protein kinase that plays a role in a variety of different signaling pathways including cytoskeleton regulation, cell migration, or cell cycle regulation. Plays a role in dendrite spine morphogenesis as well as synapse formation and plasticity. Acts as downstream effector of the small GTPases CDC42 and RAC1. Activation by the binding of active CDC42 and RAC1 results in a conformational change and a subsequent autophosphorylation on several serine and/or threonine residues. Phosphorylates MAPK4 and MAPK6 and activates the downstrea [...] (544 aa)
Zfp64	Zinc finger protein 64, isoform cra_b; May be involved in transcriptional regulation (676 aa)
Hr	Lysine demethylase and nuclear receptor corepressor; Lysine-specific demethylase hairless; Histone demethylase that specifically demethylates both mono- and dimethylated 'Lys-9' of histone H3. May act as a transcription regulator controlling hair biology (via targeting of collagens), neural activity, and cell cycle (By similarity) (1182 aa)
Kcne1l	Potassium voltage-gated channel, isk-related family, member 1-like, pseudogene; Potassium voltage-gated channel subfamily E regulatory beta subunit 5; Potassium channel ancillary subunit that is essential for generation of some native K(+) currents by virtue of formation of heteromeric ion channel complex with voltage-gated potassium (Kv) channel pore-forming alpha subunits. Functions as an inhibitory beta-subunit of the repolarizing cardiac potassium ion channel KCNQ1 (143 aa)
Lrrtm2	Leucine-rich repeat transmembrane neuronal protein 2; Involved in the development and maintenance of excitatory synapse in the vertebrate nervous system. Regulates surface expression of AMPA receptors and instructs the development of functional glutamate release sites. Acts as a ligand for the presynaptic receptors NRXN1-A and NRXN1-B (By similarity) (515 aa)
Ctsa	Cathepsin a (carboxypeptidase c); Lysosomal protective protein; Protective protein appears to be essential for both the activity of beta-galactosidase and neuraminidase, it associates with these enzymes and exerts a protective function necessary for their stability and activity. This protein is also a carboxypeptidase and can deamidate tachykinins (474 aa)
Car3	Carbonic anhydrase 3; Reversible hydration of carbon dioxide (260 aa)
Prrg3	Proline rich Gla (G-carboxyglutamic acid) 3 (transmembrane) (231 aa)
Mmp14	Matrix metalloproteinase-14 (membrane-inserted); Matrix metalloproteinase-14; Endopeptidase that degrades various components of the extracellular matrix such as collagen. Activates progelatinase A. Essential for pericellular collagenolysis and modeling of skeletal and extraskeletal connective tissues during development. May be involved in actin cytoskeleton reorganization by cleaving PTK7 (By similarity). Acts as a

	positive regulator of cell growth and migration via activation of MMP15. Involved in the formation of the fibrovascular tissues (By similarity). Cleaves ADGRB1 to release va [...] (582 aa)
Figf	Vascular endothelial growth factor D; Growth factor active in angiogenesis, lymphangiogenesis and endothelial cell growth, stimulating their proliferation and migration and also has effects on the permeability of blood vessels. May function in the formation of the venous and lymphatic vascular systems during embryogenesis, and also in the maintenance of differentiated lymphatic endothelium in adults. Binds and activates VEGFR-3 (Flt4) receptor (358 aa)
Tmem80	Transmembrane protein 80 (123 aa)
Alox12b	Arachidonate 12-lipoxygenase, 12R-type; Non-heme iron-containing dioxygenase that catalyzes the stereo-specific peroxidation of free and esterified polyunsaturated fatty acids generating a spectrum of bioactive lipid mediators. Mainly converts arachidonic acid to (12R)- hydroperoxyeicosatetraenoic acid/(12R)-HPETE and minor stereoisomers. In the skin, acts upstream of ALOXE3 on the lineolate moiety of esterified omega-hydroxyacyl-sphingosine (EOS) ceramides to produce an epoxy-ketone derivative, a crucial step in the conjugation of omega-hydroxyceramide to membrane proteins. Therefore [...] (701 aa)
Gabra3	Gamma-aminobutyric acid receptor subunit alpha-3; GABA, the major inhibitory neurotransmitter in the vertebrate brain, mediates neuronal inhibition by binding to the GABA/benzodiazepine receptor and opening an integral chloride channel; Belongs to the ligand-gated ion channel (TC 1.A.9) family. Gamma-aminobutyric acid receptor (TC 1.A.9.5) subfamily. GABRA3 sub-subfamily (492 aa)
Crebrf	CREB3 regulatory factor; Acts as a negative regulator of the endoplasmic reticulum stress response or unfolded protein response (UPR). Represses the transcriptional activity of CREB3 during the UPR. Recruits CREB3 into nuclear foci (By similarity) (640 aa)
Ramp1	Receptor activity-modifying protein 1; Transports the calcitonin gene-related peptide type 1 receptor (CALCRL) to the plasma membrane. Acts as a receptor for calcitonin-gene-related peptide (CGRP) together with CALCRL; Belongs to the RAMP family (148 aa)
Morc4	MORC family CW-type zinc finger protein 4; Microrchidia 4 (883 aa)
Lipg	Endothelial lipase; Has phospholipase and triglyceride lipase activities. Hydrolyzes high density lipoproteins (HDL) more efficiently than other lipoproteins. Binds heparin (By similarity) (500 aa)
Agpat4	1-acylglycerol-3-phosphate O-acyltransferase 4 (lysophosphatidic acid acyltransferase, delta); 1-acyl-sn-glycerol-3-phosphate acyltransferase delta; Converts lysophosphatidic acid (LPA) into phosphatidic acid by incorporating an acyl moiety at the sn-2 position of the glycerol backbone; Belongs to the 1-acyl-sn-glycerol-3-phosphate acyltransferase family (378 aa)
Lrp10	Low-density lipoprotein receptor-related protein 10; Probable receptor, which is involved in the internalization of lipophilic molecules and/or signal transduction. May be involved in the uptake of lipoprotein APOE in liver (713 aa)
Ankrd26	Ankyrin repeat domain 26; Acts as a regulator of adipogenesis. Involved in the regulation of the feeding behavior (1681 aa)
Npepl1	Probable aminopeptidase NPEPL1; Probably catalyzes the removal of unsubstituted N- terminal amino acids from various peptides (524 aa)
Cpm	Carboxypeptidase M; Specifically removes C-terminal basic residues (Arg or Lys) from peptides and proteins. It is believed to play important roles in the control of peptide hormone and growth factor activity at the cell surface, and in the membrane-localized degradation of extracellular proteins (By similarity) (443 aa)
Prpf40b	Pre-mRNA-processing factor 40 homolog B; May be involved in pre-mRNA splicing; Belongs to the PRPF40 family (873 aa)

607

References

Abboud D, Daly AF, Dupuis N, Bahri MA, Inoue A, Chevigne A, Ectors F, Plenevaux A, Pirotte B, Beckers A, Hanson J (2020) GPR101 drives growth hormone hypersecretion and gigantism in mice via constitutive activation of Gs and Gq/11. Nature communications 11, 4752

Acs P, Bauer PO, Mayer B, Bera T, Macallister R, Mezey E, Pastan I (2015) A novel form of ciliopathy underlies hyperphagia and obesity in Ankrd26 knockout mice. Brain Struct Funct 220, 1511-1528

Akiyama M, Okada Y, Kanai M, Takahashi A, Momozawa Y, Ikeda M, Iwata N, Ikegawa S, Hirata M, Matsuda K, Iwasaki M, Yamaji T, Sawada N, Hachiya T, Tanno K, Shimizu A, Hozawa A, Minegishi N, Tsugane S, Yamamoto M, Kubo M, Kamatani Y (2017) Genome-wide association study identifies 112 new loci for body mass index in the Japanese population. Nature genetics 49, 1458-1467

Atagi Y, Liu CC, Painter MM, Chen XF, Verbeeck C, Zheng H, Li X, Rademakers R, Kang SS, Xu H, Younkin S, Das P, Fryer JD, Bu G (2015) Apolipoprotein E Is a Ligand for Triggering Receptor Expressed on Myeloid Cells 2 (TREM2). The Journal of biological chemistry 290, 26043-26050

Bagnol D (2010) Use of gpr101 receptor in methods to identify modulators of hypothalamic proopiomelanocortin (POMC)-derived biologically active peptide secretion useful in the treatment of pomc-derived biologically active peptide-related disorders,US Patent Office (USPTO), U.S. patent No: 2010:1–80.

Barazzoni R, Gortan Cappellari G, Ragni M, Nisoli E (2018) Insulin resistance in obesity: an overview of fundamental alterations. Eat Weight Disord 23, 149-157

Bates B, Zhang L, Nawoschik S, Kodangattil S, Tseng E, Kopsco D, Kramer A, Shan Q, Taylor N, Johnson J, Sun Y, Chen HM, Blatcher M, Paulsen JE, Pausch MH (2006) Characterization of Gpr101 expression and G-protein coupling selectivity. Brain Res 1087, 1-14

Bera TK, Liu XF, Yamada M, Gavrilova O, Mezey E, Tessarollo L, Anver M, Hahn Y, Lee B, Pastan I (2008) A model for obesity and gigantism due to disruption of the Ankrd26 gene. Proceedings of the National Academy of Sciences of the United States of America 105, 270-275

Boche D, Gordon MN (2022) Diversity of transcriptomic microglial phenotypes in aging and Alzheimer's disease. Alzheimers Dement 18, 360-376

Charles-Messance H, Mitchelson KAJ, De Marco Castro E, Sheedy FJ, Roche HM (2020) Regulating metabolic inflammation by nutritional modulation. The Journal of allergy and clinical immunology 146, 706-720

Chen EY, Tan CM, Kou Y, Duan Q, Wang Z, Meirelles GV, Clark NR, Ma'ayan A (2013) Enrichr: interactive and collaborative HTML5 gene list enrichment analysis tool. BMC Bioinformatics 14, 128

De Souza CT, Araujo EP, Bordin S, Ashimine R, Zollner RL, Boschero AC, Saad MJ, Velloso LA (2005) Consumption of a fat-rich diet activates a proinflammatory response and induces insulin resistance in the hypothalamus. Endocrinology 146, 4192-4199

Fernandez-Arjona MDM, Leon-Rodriguez A, Grondona JM, Lopez-Avalos MD (2022) Long-term priming of hypothalamic microglia is associated with energy balance disturbances under diet-induced obesity. Glia 70, 1734-1761

Flak MB, Koenis DS, Sobrino A, Smith J, Pistorius K, Palmas F, Dalli J (2020) GPR101 mediates the pro-resolving actions of RvD5n-3 DPA in arthritis and infections. J Clin Invest 130, 359-373

Folick A, Koliwad SK, Valdearcos M (2021) Microglial Lipid Biology in the Hypothalamic Regulation of Metabolic Homeostasis. Front Endocrinol (Lausanne) 12, 668396

Fuchs H, Aguilar-Pimentel JA, Amarie OV, Becker L, Calzada-Wack J, Cho YL, Garrett L, Holter SM, Irmler M, Kistler M, Kraiger M, Mayer-Kuckuk P, Moreth K, Rathkolb B, Rozman J, da Silva Buttkus P, Treise I, Zimprich A, Gampe K, Hutterer C, Stoger C, Leuchtenberger S, Maier H, Miller M, Scheideler A, Wu M, Beckers J, Bekeredjian R, Brielmeier M, Busch DH, Klingenspor M, Klopstock T, Ollert M, Schmidt-Weber C, Stoger T, Wolf E, Wurst W, Yildirim AO, Zimmer A, Gailus-Durner V, Hrabe de Angelis M (2018) Understanding gene functions and disease mechanisms: Phenotyping pipelines in the German Mouse Clinic. Behavioural brain research 352, 187-196

Fuchs H, Gailus-Durner V, Adler T, Pimentel JA, Becker L, Bolle I, Brielmeier M, Calzada-Wack J, Dalke C, Ehrhardt N, Fasnacht N, Ferwagner B, Frischmann U, Hans W, Holter SM, Holzlwimmer G, Horsch M,

Javaheri A, Kallnik M, Kling E, Lengger C, Maier H, Mossbrugger I, Morth C, Naton B, Noth U, Pasche B, Prehn C, Przemeck G, Puk O, Racz I, Rathkolb B, Rozman J, Schable K, Schreiner R, Schrewe A, Sina C, Steinkamp R, Thiele F, Willershauser M, Zeh R, Adamski J, Busch DH, Beckers J, Behrendt H, Daniel H, Esposito I, Favor J, Graw J, Heldmaier G, Hofler H, Ivandic B, Katus H, Klingenspor M, Klopstock T, Lengeling A, Mempel M, Muller W, Neschen S, Ollert M, Quintanilla-Martinez L, Rosenstiel P, Schmidt J, Schreiber S, Schughart K, Schulz H, Wolf E, Wurst W, Zimmer A, Hrabe de Angelis M (2009) The German Mouse Clinic: a platform for systemic phenotype analysis of mouse models. Curr Pharm Biotechnol 10, 236-243

Garrett L, Chang YJ, Niedermeier KM, Heermann T, Enard W, Fuchs H, Gailus-Durner V, Angelis MH, Huttner WB, Wurst W, Holter SM (2020) A truncating Aspm allele leads to a complex cognitive phenotype and region-specific reductions in parvalbuminergic neurons. Translational psychiatry 10, 66

Garrett L, Lie DC, Hrabe de Angelis M, Wurst W, Holter SM (2012) Voluntary wheel running in mice increases the rate of neurogenesis without affecting anxiety-related behaviour in single tests. BMC neuroscience 13, 61

Garrett L, Ung MC, Heermann T, Niedermeier KM, Holter S (2018) Analysis of Neuropsychiatric Disease-Related Functional Neuroanatomical Markers in Mice. Current protocols in mouse biology 8, 79-128

Gibbons AS, Thomas EA, Scarr E, Dean B (2010) Low Density Lipoprotein Receptor-Related Protein and Apolipoprotein E Expression is Altered in Schizophrenia. Frontiers in psychiatry 1, 19

Gregg EW, Hora I, Benoit SR (2019) Resurgence in Diabetes-Related Complications. JAMA 321, 1867-1868

Heermann T, Garrett L, Wurst W, Fuchs H, Gailus-Durner V, Hrabe de Angelis M, Graw J, Holter SM (2019) Crybb2 Mutations Consistently Affect Schizophrenia Endophenotypes in Mice. Molecular neurobiology 56, 4215-4230

Herman JP, McKlveen JM, Ghosal S, Kopp B, Wulsin A, Makinson R, Scheimann J, Myers B (2016) Regulation of the Hypothalamic-Pituitary-Adrenocortical Stress Response. Compr Physiol 6, 603-621

Holter SM, Einicke J, Sperling B, Zimprich A, Garrett L, Fuchs H, Gailus-Durner V, Hrabe de Angelis M, Wurst W (2015) Tests for Anxiety-Related Behavior in Mice. Current protocols in mouse biology 5, 291-309

Jao J, Ciernia AV (2021) MGEnrichment: A web application for microglia gene list enrichment analysis. PLoS Comput Biol 17, e1009160

Jeong DY, Song N, Yang HR, Tu TH, Park BS, Kang H, Park JW, Lee BJ, Yang S, Kim JG (2021) Deficiency of Tristetraprolin Triggers Hyperthermia through Enhancing Hypothalamic Inflammation. International journal of molecular sciences 22

Jeong W, Lee H, Cho S, Seo J (2019) ApoE4-Induced Cholesterol Dysregulation and Its Brain Cell Type-Specific Implications in the Pathogenesis of Alzheimer's Disease. Mol Cells 42, 739-746

Kallnik M, Elvert R, Ehrhardt N, Kissling D, Mahabir E, Welzl G, Faus-Kessler T, de Angelis MH, Wurst W, Schmidt J, Holter SM (2007) Impact of IVC housing on emotionality and fear learning in male C3HeB/FeJ and C57BL/6J mice. Mamm Genome 18, 173-186

Keren-Shaul H, Spinrad A, Weiner A, Matcovitch-Natan O, Dvir-Szternfeld R, Ulland TK, David E, Baruch K, Lara-Astaiso D, Toth B, Itzkovitz S, Colonna M, Schwartz M, Amit I (2017) A Unique Microglia Type Associated with Restricting Development of Alzheimer's Disease. Cell 169, 1276-1290 e1217

Kettenmann H, Hanisch UK, Noda M, Verkhratsky A (2011) Physiology of microglia. Physiol Rev 91, 461-553

Kleinberger G, Yamanishi Y, Suarez-Calvet M, Czirr E, Lohmann E, Cuyvers E, Struyfs H, Pettkus N, Wenninger-Weinzierl A, Mazaheri F, Tahirovic S, Lleo A, Alcolea D, Fortea J, Willem M, Lammich S, Molinuevo JL, Sanchez-Valle R, Antonell A, Ramirez A, Heneka MT, Sleegers K, van der Zee J, Martin JJ, Engelborghs S, Demirtas-Tatlidede A, Zetterberg H, Van Broeckhoven C, Gurvit H, Wyss-Coray T, Hardy J, Colonna M, Haass C (2014) TREM2 mutations implicated in neurodegeneration impair cell surface transport and phagocytosis. Science translational medicine 6, 243ra286

Kothari V, Luo Y, Tornabene T, O'Neill AM, Greene MW, Geetha T, Babu JR (2017) High fat diet induces brain insulin resistance and cognitive impairment in mice. Biochim Biophys Acta Mol Basis Dis 1863, 499-508

Lee DK, Nguyen T, Lynch KR, Cheng R, Vanti WB, Arkhitko O, Lewis T, Evans JF, George SR, O'Dowd BF (2001) Discovery and mapping of ten novel G protein-coupled receptor genes. Gene 275, 83-91
Marschallinger J, Iram T, Zardeneta M, Lee SE, Lehallier B, Haney MS, Pluvinage JV, Mathur V, Hahn O, Morgens DW, Kim J, Tevini J, Felder TK, Wolinski H, Bertozzi CR, Bassik MC, Aigner L, Wyss-Coray T (2020) Lipid-droplet-accumulating microglia represent a dysfunctional and proinflammatory state in the aging brain. Nature neuroscience 23, 194-208
Mendes NF, Kim YB, Velloso LA, Araujo EP (2018) Hypothalamic Microglial Activation in Obesity: A Mini-Review. Frontiers in neuroscience 12, 846
Morrison HW, Filosa JA (2013) A quantitative spatiotemporal analysis of microglia morphology during ischemic stroke and reperfusion. J Neuroinflammation 10, 4
Ngo T, Kufareva I, Coleman J, Graham RM, Abagyan R, Smith NJ (2016) Identifying ligands at orphan GPCRs: current status using structure-based approaches. Br J Pharmacol 173, 2934-2951
Nilaweera KN, Ozanne D, Wilson D, Mercer JG, Morgan PJ, Barrett P (2007) G protein-coupled receptor 101 mRNA expression in the mouse brain: altered expression in the posterior hypothalamus and amygdala by energetic challenges. J Neuroendocrinol 19, 34-45
Nilaweera KN, Wilson D, Bell L, Mercer JG, Morgan PJ, Barrett P (2008) G protein-coupled receptor 101 mRNA expression in supraoptic and paraventricular nuclei in rat hypothalamus is altered by pregnancy and lactation. Brain Res 1193, 76-83
Paul EJ, Tossell K, Ungless MA (2019) Transcriptional profiling aligned with in situ expression image analysis reveals mosaically expressed molecular markers for GABA neuron sub-groups in the ventral tegmental area. The European journal of neuroscience 50, 3732-3749
Rathkolb B, Fuchs H, Gailus-Durner V, Aigner B, Wolf E, Hrabe de Angelis M (2013a) Blood Collection from Mice and Hematological Analyses on Mouse Blood. Current protocols in mouse biology 3, 101-119
Rathkolb B, Hans W, Prehn C, Fuchs H, Gailus-Durner V, Aigner B, Adamski J, Wolf E, Hrabe de Angelis M (2013b) Clinical Chemistry and Other Laboratory Tests on Mouse Plasma or Serum. Current protocols in mouse biology 3, 69-100
Rodd C, Millette M, Iacovazzo D, Stiles CE, Barry S, Evanson J, Albrecht S, Caswell R, Bunce B, Jose S, Trouillas J, Roncaroli F, Sampson J, Ellard S, Korbonits M (2016) Somatic GPR101 Duplication Causing X-Linked Acrogigantism (XLAG)-Diagnosis and Management. J Clin Endocrinol Metab 101, 1927-1930
Ross EA, Naylor AJ, O'Neil JD, Crowley T, Ridley ML, Crowe J, Smallie T, Tang TJ, Turner JD, Norling LV, Dominguez S, Perlman H, Verrills NM, Kollias G, Vitek MP, Filer A, Buckley CD, Dean JL, Clark AR (2017) Treatment of inflammatory arthritis via targeting of tristetraprolin, a master regulator of pro-inflammatory gene expression. Ann Rheum Dis 76, 612-619
Saeedi P, Petersohn I, Salpea P, Malanda B, Karuranga S, Unwin N, Colagiuri S, Guariguata L, Motala AA, Ogurtsova K, Shaw JE, Bright D, Williams R, Committee IDFDA (2019) Global and regional diabetes prevalence estimates for 2019 and projections for 2030 and 2045: Results from the International Diabetes Federation Diabetes Atlas, 9(th) edition. Diabetes Res Clin Pract 157, 107843
Saito T, Kuma A, Sugiura Y, Ichimura Y, Obata M, Kitamura H, Okuda S, Lee HC, Ikeda K, Kanegae Y, Saito I, Auwerx J, Motohashi H, Suematsu M, Soga T, Yokomizo T, Waguri S, Mizushima N, Komatsu M (2019) Autophagy regulates lipid metabolism through selective turnover of NCoR1. Nature communications 10, 1567
Sharma R, Luong Q, Sharma VM, Harberson M, Harper B, Colborn A, Berryman DE, Jessen N, Jorgensen JOL, Kopchick JJ, Puri V, Lee KY (2018) Growth hormone controls lipolysis by regulation of FSP27 expression. The Journal of endocrinology 239, 289-301
Steuernagel L, Lam BYH, Klemm P, Dowsett GKC, Bauder CA, Tadross JA, Hitschfeld TS, Del Rio Martin A, Chen W, de Solis AJ, Fenselau H, Davidsen P, Cimino I, Kohnke SN, Rimmington D, Coll AP, Beyer A, Yeo GSH, Bruning JC (2022) HypoMap-a unified single-cell gene expression atlas of the murine hypothalamus. Nat Metab 4, 1402-1419
Szklarczyk D, Gable AL, Lyon D, Junge A, Wyder S, Huerta-Cepas J, Simonovic M, Doncheva NT, Morris JH, Bork P, Jensen LJ, Mering CV (2019) STRING v11: protein-protein association networks with

762 increased coverage, supporting functional discovery in genome-wide experimental datasets. Nucleic
763 Acids Res 47, D607-D613
764 Tiberi M, Chiurchiu V (2021) Specialized Pro-resolving Lipid Mediators and Glial Cells: Emerging
765 Candidates for Brain Homeostasis and Repair. Frontiers in cellular neuroscience 15, 673549
766 Trivellin G, Bjelobaba I, Daly AF, Larco DO, Palmeira L, Faucz FR, Thiry A, Leal LF, Rostomyan L, Quezado
767 M, Schernthaner-Reiter MH, Janjic MM, Villa C, Wu TJ, Stojilkovic SS, Beckers A, Feldman B, Stratakis
768 CA (2016) Characterization of GPR101 transcript structure and expression patterns. J Mol Endocrinol
769 57, 97-111
770 Trivellin G, Daly AF, Faucz FR, Yuan B, Rostomyan L, Larco DO, Schernthaner-Reiter MH, Szarek E, Leal
771 LF, Caberg JH, Castermans E, Villa C, Dimopoulos A, Chittiboina P, Xekouki P, Shah N, Metzger D, Lysy
772 PA, Ferrante E, Strebkova N, Mazerkina N, Zatelli MC, Lodish M, Horvath A, de Alexandre RB, Manning
773 AD, Levy I, Keil MF, Sierra Mde L, Palmeira L, Coppieters W, Georges M, Naves LA, Jamar M, Bours V,
774 Wu TJ, Choong CS, Bertherat J, Chanson P, Kamenicky P, Farrell WE, Barlier A, Quezado M, Bjelobaba
775 I, Stojilkovic SS, Wess J, Costanzi S, Liu P, Lupski JR, Beckers A, Stratakis CA (2014) Gigantism and
776 acromegaly due to Xq26 microduplications and GPR101 mutation. The New England journal of
777 medicine 371, 2363-2374
778 Trotta M, Bello EP, Alsina R, Tavella MB, Ferran JL, Rubinstein M, Bumaschny VF (2020) Hypothalamic
779 Pomc expression restricted to GABAergic neurons suppresses Npy overexpression and restores food
780 intake in obese mice. Mol Metab 37, 100985
781 Ulrich JD, Holtzman DM (2016) TREM2 Function in Alzheimer's Disease and Neurodegeneration. ACS
782 Chem Neurosci 7, 420-427
783 Ung MC, Garrett L, Dalke C, Leitner V, Dragosa D, Hladik D, Neff F, Wagner F, Zitzelsberger H, Miller G,
784 de Angelis MH, Rossler U, Vogt Weisenhorn D, Wurst W, Graw J, Holter SM (2021) Dose-dependent
785 long-term effects of a single radiation event on behaviour and glial cells. Int J Radiat Biol 97, 156-169
786 Valdearcos M, Douglass JD, Robblee MM, Dorfman MD, Stifler DR, Bennett ML, Gerritse I, Fasnacht R,
787 Barres BA, Thaler JP, Koliwad SK (2017) Microglial Inflammatory Signaling Orchestrates the
788 Hypothalamic Immune Response to Dietary Excess and Mediates Obesity Susceptibility. Cell
789 metabolism 26, 185-197 e183
790 Valdearcos M, Robblee MM, Benjamin DI, Nomura DK, Xu AW, Koliwad SK (2014) Microglia dictate the
791 impact of saturated fat consumption on hypothalamic inflammation and neuronal function. Cell
792 reports 9, 2124-2138
793 Wacker D, Stevens RC, Roth BL (2017) How Ligands Illuminate GPCR Molecular Pharmacology. Cell 170,
794 414-427

795

Figure 1

FIGURE 1

Click here to access/download;Figure;Figure 1_12.12.22.pdf

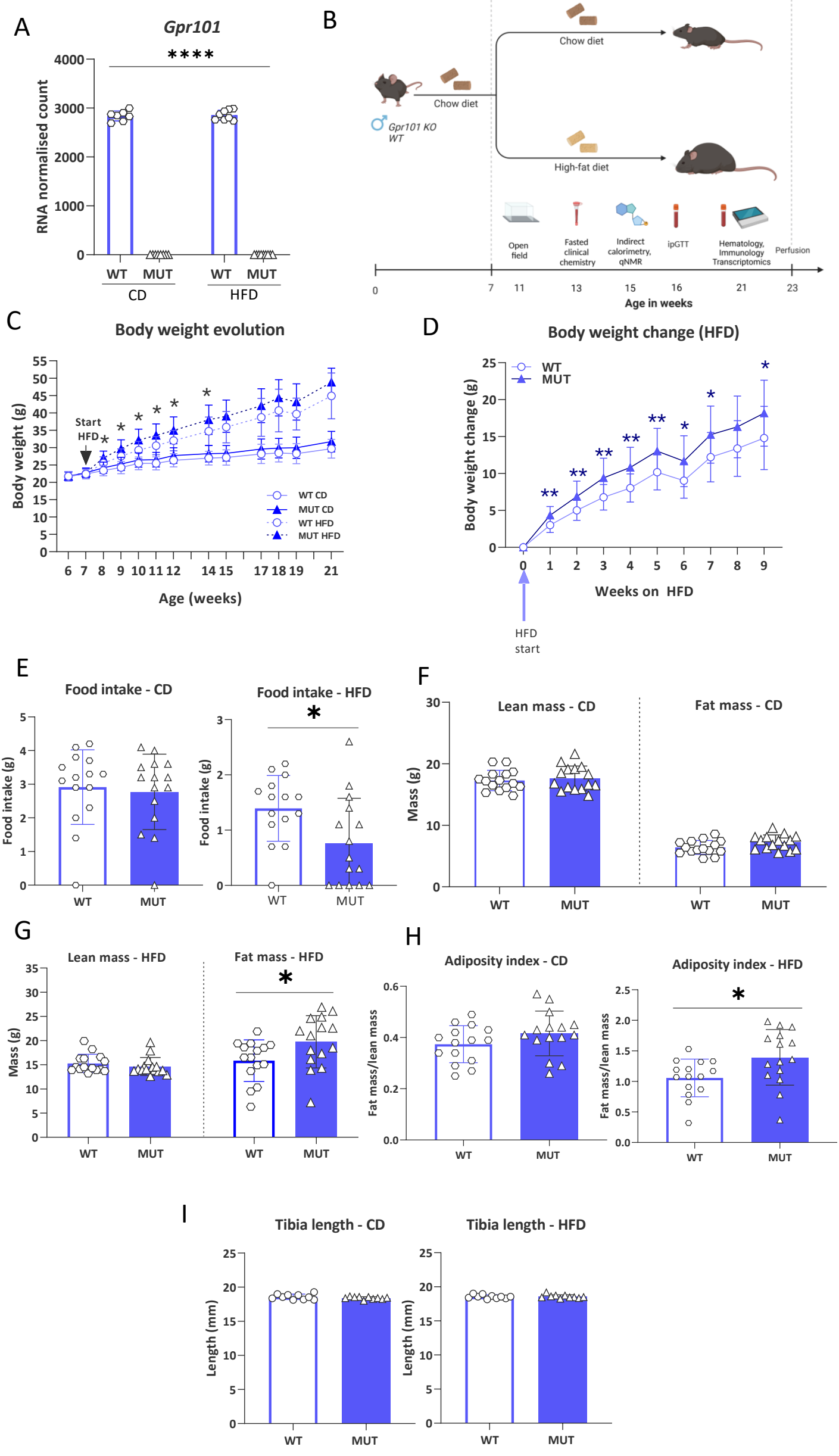

Figure 2

FIGURE 2

Click here to access/download;Figure;Figure 2_12.12.22.pdf

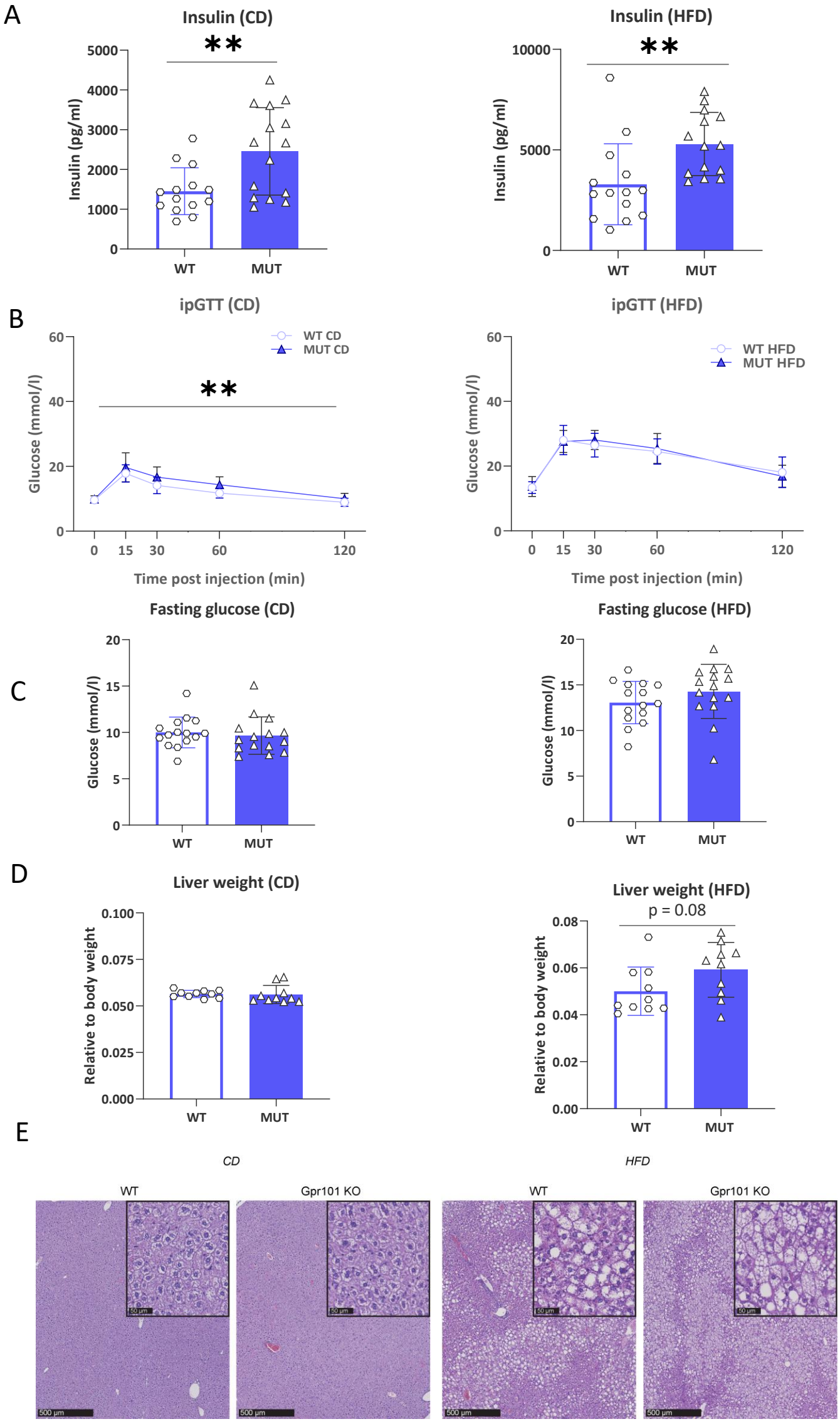

Figure 3

Click here to access/download;Figure;Figure 3_12.12.22.pdf

FIGURE 3

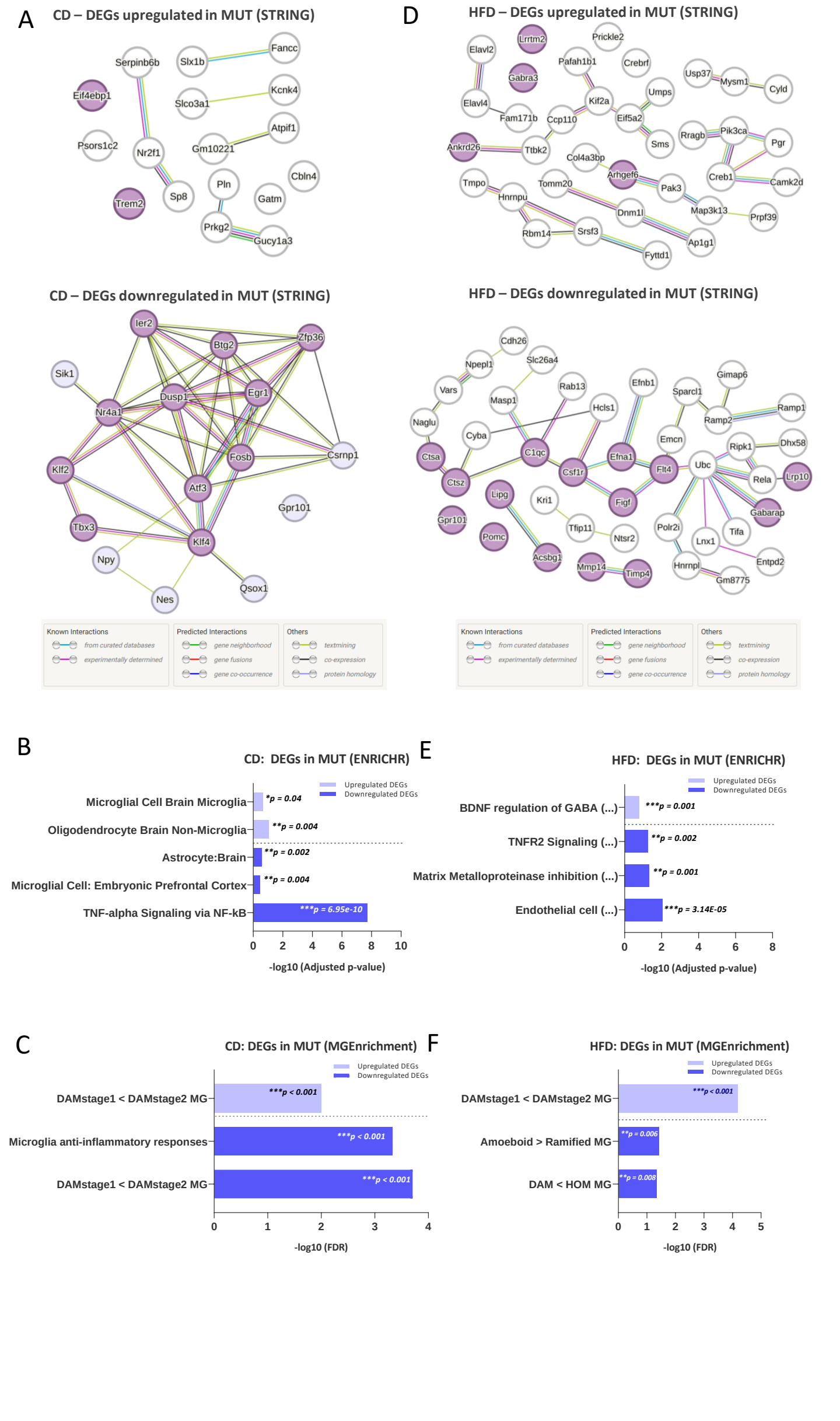

FIGURE 4

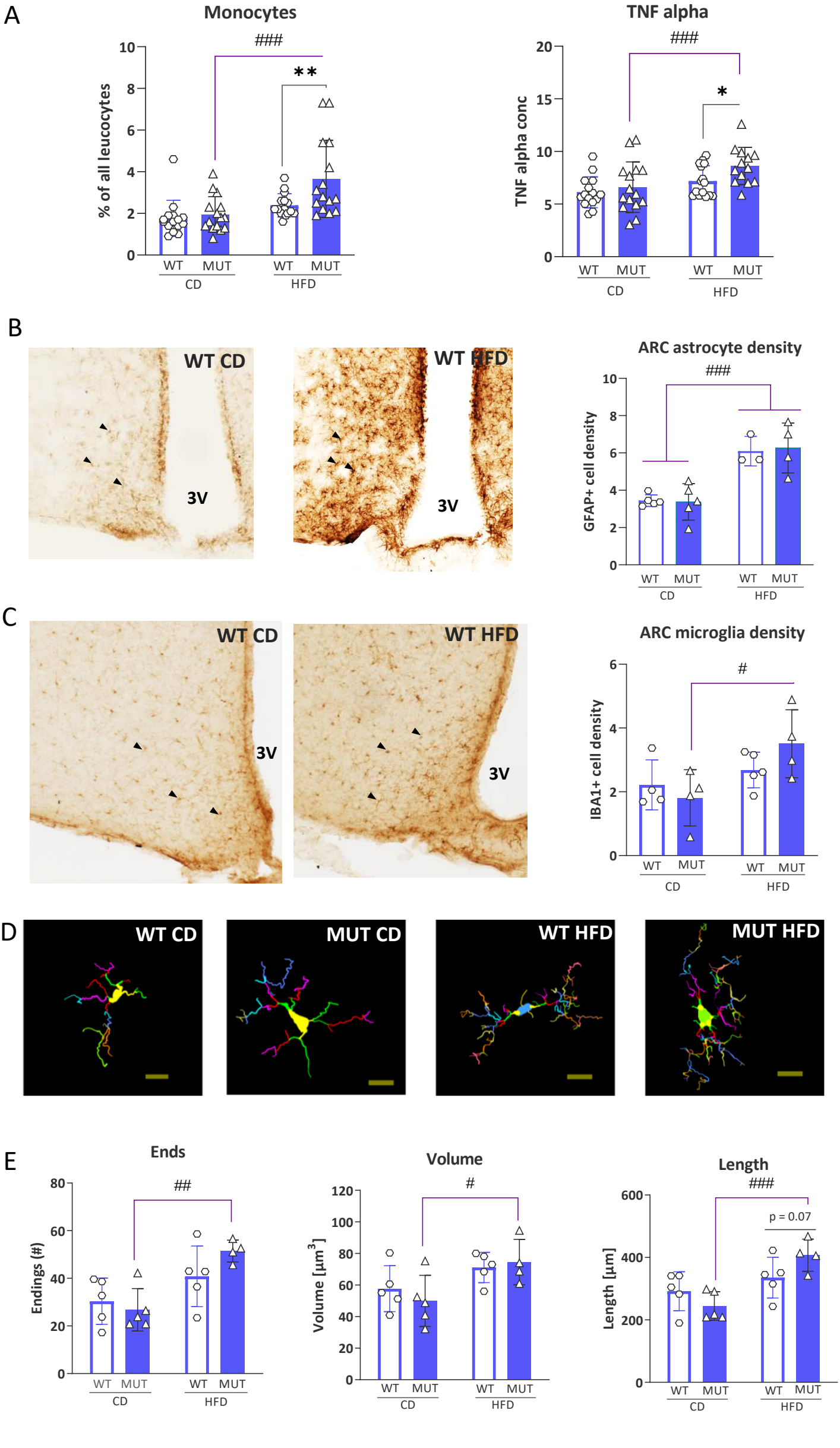

Supplementary information gene lists

Click here to access/download

Supplementary Material

Supplementary information gene lists_12.12.22.xlsx

Supplementary information enrichment results

Click here to access/download

Supplementary Material

Supplementary information_Enrichment_12.12.22.xlsx